ANALYSIS OF OXIDATION AND REPAIR OF METHIONINES IN CATALASE OF *HELICOBACTER PYLORI*

by

VILINH THI TRAN

(Under the Direction of Joshua S. Sharp)

ABSTRACT

Reactive oxygen species (ROS) such as hypochlorous acid (HOCl) and hydrogen peroxide (H_2O_2) selectively oxidize amino acid residues in proteins leading to loss of enzymatic activity. *Helicobacter pylori* (*H. pylori*), a microaerophilic bacterium involved in the cause of stomach ulcers, has a unique ability to survive under high levels of oxidative stress. Catalase of *H. pylori* plays a major role in defense from oxidative stress naturally occurring in the human body. The loss of catalase activity due to oxidative damage renders the bacterium more vulnerable to further damage. To protect itself from oxidative stress, the *H. pylori* bacterium produces an enzyme called methionine sulfoxide reductase (Msr), which reductively repairs methionine sulfoxide to its native form. Since methionine residues of pathogens are the major targets of oxidation, the Msr targets only the damaged methionines caused by oxidative stress. With the help of mass spectrometry, identification and quantification of specific methionines being repaired in *H. pylori* catalase was determined by comparing the percent of oxidation of each methionine residue.

INDEX WORDS: methionine sulfoxide reductase, Helicobacter pylori, catalase, data dependant analysis, pseudo-MRM, oxidative stress, LC-MS/MS

ANALYSIS OF OXIDATION AND REPAIR OF METHIONINES IN CATALASE OF *HELICOBACTER PYLORI*

by

VILINH THI TRAN

B.S. Georgia State University, 2007

A Thesis Submitted to the Graduate Faculty of The University of Georgia in Partial Fulfillment of the Requirements for the Degree

MASTER OF SCIENCE

ATHENS, GEORGIA

2010

ANALYSIS OF OXIDATION AND REPAIR OF METHIONINES IN CATALASE OF *HELICOBACTER PYLORI*

by

VILINH THI TRAN

Major Professor: Joshua S. Sharp
Committee: Ron Orlando
Jon Amster

Electronic Version Approved:

Maureen Grasso
Dean of the Graduate School
The University of Georgia
December 2010

ACKNOWLEDGEMENTS

I would like to acknowledge my parents for giving me the opportunity to pursue the path in the scientific world. I am also very appreciative of all my friends that have supported me during my graduate studies here at the University of Georgia. I know in the future, even though we may separate from each other, we will still be good friends and always there ready to give each other advices. I would also like to extend my gratitude to all the professors and mentors that have helped me along my academic journey especially my committee members: Dr. Joshua Sharp, Dr. Ron Orlando, and Dr. Jon Amster. Dr. Joshua Sharp has helped me with many aspects of my research. With his skills and knowledge, I have learned to think in a different and critical way. I have also learned so much about a variety of different instruments. I would also like to thank our collaborators, Manish Mahawar and Dr. Rob Maier, for including me in their research. I am also thankful for all the samples they supplied for this research project. I would also like to acknowledge a mentor and a friend, Jesse Hines. He has given me great advice and support with my research.

TABLE OF CONTENTS

Page

CHAPTER 1

LITERATURE REVIEW

Every living organism faces damages from oxidative stress as part of its cellular metabolism. Oxidative stress occurs from an imbalance between oxidants and antioxidants, favoring the oxidants. Some of the known causes of the increase amounts of oxidants originate from the introduction of external or cellular sources such as radiation and inflammatory cells. Oxidative stress causes mutations and damages to the cell which leads to loss of enzymatic functions and will eventually lead to cell death under further oxidative damage. Some of the diseases that are associated with oxidative stress includes Alzheimer's disease, Parkinson's disease, Huntington's disease, and amyotrophic lateral sclerosis[1]. Reactive oxygen species (ROS) such as hypochlorite ($^{-}$OCl), hydrogen peroxide (H_2O_2), and hydroxyl radical ($^{\cdot}$OH) oxidizes amino acid residues along with the proteins, especially the sulfur centers of methionine side chains[2]. In order to protect the cell against oxidative stress, antioxidant enzyme such as catalase and superoxide dismutase are produced within the cell to prevent further damage [3]. Another defense mechanism against oxidative stress is by reductively repairing the damaged cell to its native form with the aid of an enzyme called methionine sulfoxide reductase (Msr). In this thesis, mass spectrometry was used to analyze oxidation and repair by methionine sulfoxide reductase in *Helicobacter pylori* (*H. pylori*) catalase.

Helicobacter pylori (H. pylori) is a microaerophilic bacterium commonly found in the pyloric antrum of the stomach and is linked to the development of stomach ulcers and chronic gastritis [4]. Continuous inflammation from ulcers and gastritis can lead to stomach cancer and

adenocarcinoma [5]. *H. pylori* can be found in humans of all ages and worldwide. It is transmitted in three known ways: iatrogenic (tubes and endoscopes)[6], fecal-oral [7], and oral-oral [8]. *Helicobacter pylori* was first discovered and isolated in 1982 by Dr. Barry Marshall and Dr. Robin Warren of Perth, Western Australia[9]. This bacterium is often identified by the detection of surrounding acute inflammatory phagocytes called polymorphonuclear leukocytes (PMNL)[10]. PMNL are white blood cells that protects the body against foreign particles, bacteria, and dead cells[11]. *H. pylori* releases a chemical gradient which attracts PMNL to its location by a process called chemotaxis [11]. Exposure to *H. pylori*'s surface, oxygen consumption increases in the PMNL to generate hydrogen peroxide[11-12]. A heme protein, myeloperoxidase, which is also found in PMNL reacts with hydrogen peroxide to generate hypochlorous acid. Hypochlorous acid is approximately 2-3 orders of magnitude more potent as an oxidant than hydrogen peroxide. The oxidants are then secreted outside the membrane to signal other phagocytes to the location of the targets as well as exposing the bacterium to oxidative stress, a process known as respiratory burst [12]. As a simple identification test, *H. pylori* was exposed to oxidants *in vitro* for observation of respiratory burst[10]. Interestingly, after inducing heavy oxidation from PMNL, *H. pylori* was capable of surviving in the stomach and continues to colonize [13-15].

Helicobacter pylori produces its own natural antioxidant enzymes such as superoxide dismutase (SOD), catalase (KatA), thiol peroxidase (Tpx), and alkyl hydroxyperoxidase C (AhpC) [16]. *H. pylori* catalase is a homotetrameric protein with a molecular mass of 59kDa per subunit [17]. KatA is unique compared to other catalases due to its ability to withstand high concentrations of hydrogen peroxide[18]. *H. pylori* catalase is also highly expressed and makes up approximately 1% of the cell's total protein[18]. The respiratory burst identification test

exposes both *H. pylori* and its catalase to hydrogen peroxide for observation of accumulating oxidants [15, 17-18]. Upon stimulation of hydrogen peroxide, *H. pylori* shows no signs of respiratory bursts indicating the role of catalase maintaining a stable environment for growth and the removal of hydrogen peroxide[17-18]. However, inactivation of the catalase protein will cause the bacterium to be vulnerable to oxidative stress [17].

Table 1.1. Second-order rate constants determined for the reactions of HOCl with amino acid side-chain groups, α-amino groups and backbone amides[19]

Residue	**$k_2/M^{-1}s^{-1}$**	**Residue**	**$k_2/M^{-1}s^{-1}$**
Met	3.8×10^7	**Lys**	5.0×10^3
Cys	3.0×10^7	**Tyr**	44
Cystine	1.6×10^5	**Arg**	26
His	1.0×10^5	**Backbone amides**	$< 10^a$
α-amino	1.0×10^5	**Asn**	0.03
Trp	1.1×10^4	**Gln**	0.03

[a] The second-order rate constant for backbone amides varies over several orders of magnitude, depending on the environment. This value is a maximal based on studies with cyclic dipeptides.

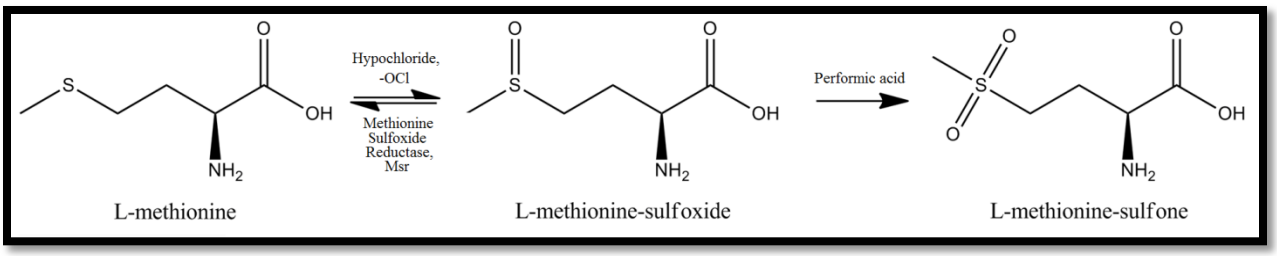

Figure 1.1. Chemical oxidation of Methionine (Met) to Methionine Sulfoxide [Met(O)] is reversible to its native form with aid from Methionine sulfoxide reductase (Msr). However, when oxidation continues to methionine sulfone, the reaction cannot be reversed [20]

Methionine, among the twenty amino acids, is very sensitive to oxidation, as seen in Table 1.1. The sensitivity is determined by second order rate constants for the reaction of HOCl[19, 21]. Oxidation of methionine residues occurs in a variety of proteins which leads to the reduction or loss of biological activity[22]. As seen in Figure 1.1, methionine (Met) is oxidized to methionine sulfoxide [Met(O)] and further to methionine sulfone under further oxidation [20]. Met(O) can be repaired back to its native form by an enzyme called methionine

sulfoxide reductase (Msr) [20, 23]. However, Msr cannot repair methionine sulfone back to Met(O)[20]. As seen in Figure 1.2, the oxidation of methionine produces two diastereoisomers, Methionine-(S)-sulfoxide (Met(S)O) and Methionine-(R)-sulfoxide (Met(R)O) [24]. The diastereoisomers are due to the asymmetric position of the single oxygen on the sulfur atom in the side chain [24-25]. These two isomers are reduced by two proteins found in the Msr system, msrA and msrB, which specifically reduces and repairs Met(S)O and Met(R)O, respectively [24-26]. The substrate specificity of Msr has a broad range and can recognize compounds containing a methyl sulfoxide group such as dimethyl sulfoxide, tetramethylene sulfoxide, and methyl p-tolyl sulfoxide [27]. However, Met(O) in proteins are the most natural substrate for Msr[2].

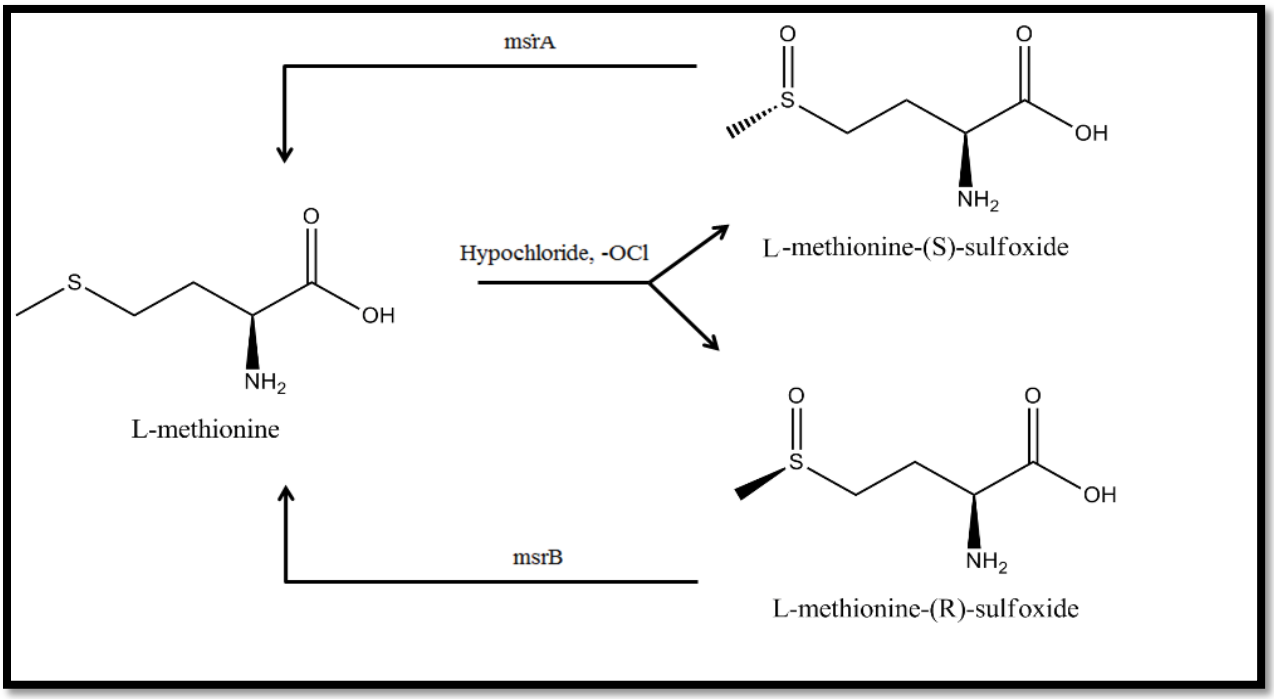

Figure 1.2. Oxidation to methionine residues produces two diastereoisomers. Reversion of Met(O) is specific with msrA repairing Met(S)O and msrB repairing Met(R)O to the native form [24].

Evidence of an enzyme repairing Met(O) to Met was first published in 1981 from *Escherichia coli (E. coli)* ribosomal protein, L12[28]. The L12 protein forms a dimer with *E. coli* 50S ribosomal subunit [29]. 50S is an essential ribosomal subunit to the cell's initiation[30-33], elongation[34-35], and termination[36] steps of protein synthesis. L12 proteins lacked amino acid residues such as histidine, tryptophan, cysteine, and tyrosine which are known to be highly susceptible to oxidation [37-38]. However, L12 contains three methionine residues which was easily oxidized to Met(O) by hydrogen peroxide and prevented formations of the ribosomal dimer[29]. As hypothesized, the inactivated L12 did not dimerize with 50S ribosomal subunit thus preventing protein synthesis [30-36]. This study prompted further search and isolation of an enzyme (methionine sulfoxide reductase, Msr) in *E. coli* that can repair methionine sulfoxide to its native form and restore biological activity [28, 39]. Methionine sulfoxide reductase is known as a ubiquitous protein and has been successfully cloned from over 20 species of bacteria, plants, insects, yeast, animals, and humans shown in Table 1.2 [40]. Msr in humans was observed to have similar sequence identity of 67% with *E. coli* and 88% with bovine enzyme[41].

Table 1.2. Species with methionine sulfoxide reductase cloned [40]

Arabidopsis thaliana	*Helicobacter pylori*
Bacillus subtilis	*Homo sapiens*
Bos Taurus	*Lycopersicon esculentum*
Brassica napus	*Mycoplasma genitalium*
Drosophilia melanogaster	*Mycoplasma pneumoniae*
Erwinia chrysanthemi	*Mycobacterium tuberculosis*
Fragaria ananassa	*Neisseria gonorrhoeae*
Gracilaria gracilis	*Schizosaccharomyces pombe*
Haemophilus influenzae	*Streptococcus pneumonia*
Escherichia coli	*Saccharomyces cereviseae*

Methionine sulfoxide reductase has many different roles including protection of cells against oxidative damage, ROS scavenger system, regulatory role, and bacterial adherence [2]. To ascertain the importance of Msr against oxidative damage, different laboratories have studied

mutant cells from *E. coli* in which the Msr gene has been inactivated[42]. The mutant was grown under normal laboratory growth conditions. Interestingly, the mutant cells were observed to be more sensitive to hydrogen peroxide than the wild type cells[42]. The Msr gene was later inserted into the mutated cell where observation of the function was restored to wild type phenotype[42]. Another role involves reversing the oxidation of the methionine residues; a temporary sink for ROS protection against oxidative stress [43-45]. Methionine sulfoxide reductase can also be found in regulating the biological activity of a protein such as the voltage-gated K^+ channel[46]. The oxidation of the methionine in the channel, paired with the reduction of methionine by Msr, acts as an on/off switch to regulate the activity of the K^+ channel[46]. Studies have also reported the involvement of the Msr enzyme in bacterial adherence in biological systems such as *Erwinia chrysanthemi*[47]. Mutant *msr* reacts with the bacteria and limits the spreading of the virulence factor, which leads to the conclusion that the virulence factor might be required in order for the bacteria to spread throughout *E. chrysanthemi*[47]. Other pathogens from humans and plants such as *Saccharomyces cereviseae*[48], *Escherichia coli*[42], and *Mycobacterium tuberculosis*[49] have also been studied to observe the role of Msr in different biological systems. All studies conclude the importance of Msr by inactivating the gene which resulted in a higher sensitivity level and became more susceptible to oxidants [2, 42-50].

H. pylori Msr is a 42kDa protein made up of two separate proteins, msrA and msrB, fused together as a single enzyme [50]. To determine the importance of Msr's role in *H. pylori* and its relation to the stomach colonization, a series of inactivation experiments were performed. The inactivation of the different domains were completed by an insertional inactivation of an antibiotic cassette[3, 23]. Two different areas of the Msr system were inactivated by the cassette.

An antibiotic cassette was inserted into the msrB gene where msrA was tested for activity (labeled as *msrB* to represent place of cassette insertion)[3, 23]. The second area included a complete inactivation of both domains and labeled as *msrA/B*[3, 23]. Inactivation with either process should exhibit an increase in the sensitivity of oxidation. The comparison of the parent strain of *H. pylori* to both mutant strains demonstrated that the mutant was affected more under oxidative stress thus not being able to continue to colonize while the parent strain had little oxidation[3]. A method used to test the sensitivity between parent and mutant strains included a procedure using disc inhibitors[3]. Each disc contained a different oxidant including paraquat, hydrogen peroxide, and s-nitrosoglutanthione[3]. As expected the mutants showed an increase in sensitivity to oxidation compared to the parent strain[3]. Interestingly, *msrB* showed more resistance than *msrA/B* when exposed to different oxidants.

Another experiment was executed to observe the oxidative stress tolerance of the parent and mutant strains. The test included measuring the ability of the non-growing cells to survive oxygen and chemical oxidants over a period of 12 hours (Figure 1.4). As shown in Figure 1.4, the parent and merodiploid (partially diploid by having a second copy of only part of its genome) strains resisted the chemical oxidation and were able to survive over a period of 12 hours even though there seemed to a decline in activity after 8 hours have passed[3]. As predicted, the mutant strain was more sensitive to chemical oxidation, showed a complete decline after 6 hours, and no cells were left afterwards for collection [3]. Similar to the disc inhibition test, *msrB* was slightly less sensitive to the chemical oxidation but not as insensitive as the parent and merodiploid strains[3].

As previously mentioned, msrA and msrB will only catalyze specifically with either methionine-S-sulfoxide or methionine-R-sulfoxide, respectively. In 2006, Alamuri et al

observed the ability of *H. pylori* Msr to reduce the two substrates (Figure 1.5) [23]. The Msr activity assays were perfromed by monitoring the oxidation of NADPH at 340nm as the concentration of substrates (Met(S)O and Met(R)O) increases[23]. *H. pylori* Msr system were observed to prefer reduction of the Met(R)O isomer. On the other hand, there were no detection of activity with Met(S)O. It was concluded that msrA domain of *H. pylori* was inactive, thus suggesting *H. pylori* was solely dependant on the msrB gene for repair[23].

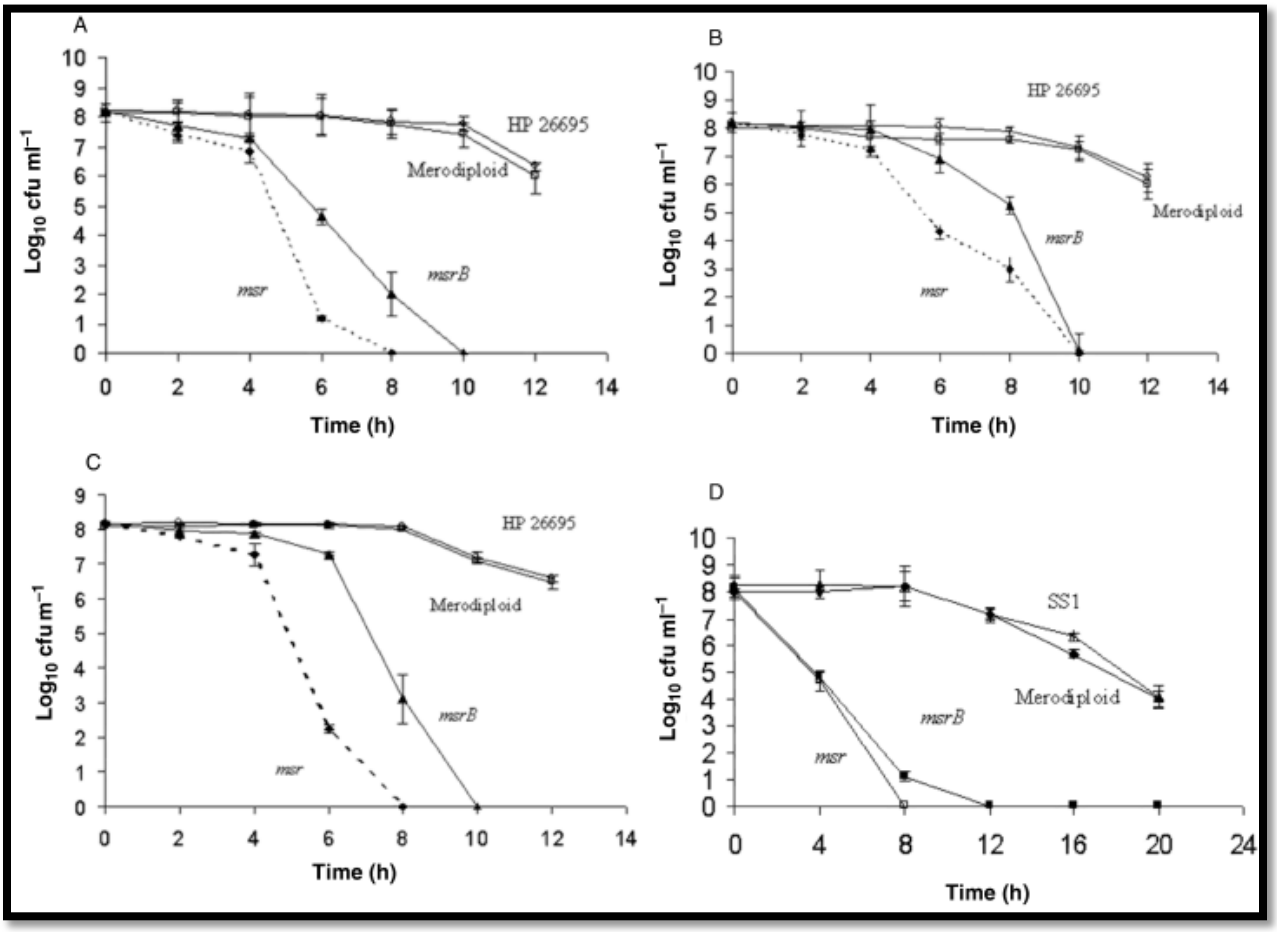

Figure 1.4. Stress tolerance of non-growing cells. Parent strain (open circles), mutant strain (dotted lines), msrB (closed triangles), and merodiploid strain (open squares) were inoculated in sterile PBS. Dilutions were observed over a 12 hour period to measure the ability of the non-growing cells to survive oxygen and chemical oxidants [3]

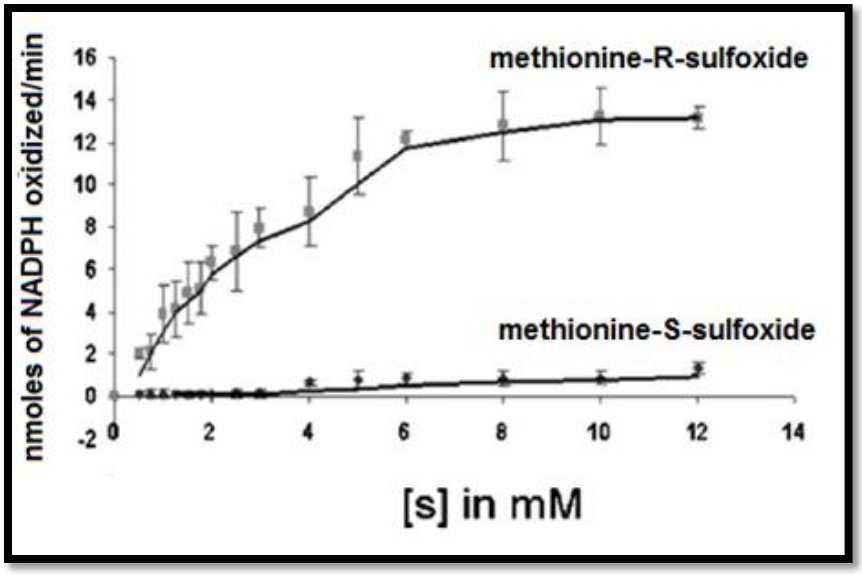

Figure 1.5. In vitro Msr activity with Met(R)O and Met(S)O. The concentration of oxidized NADPH was monitored at 340nm as a measure of substrate reduction by Msr. Values are from four separate experiments, each performed in triplicate [23]

The bacterium *H. pylori* also produces its own chaperonin, GroEL/ES[51]. GroEL/ES is known to facilitate with protein folding, unfolding, and translocation [52-57]. GroEL/ES is commonly found in bacteria and organelles of endosymbiotic origin[58]. This set of chaperonin consists of two heptameric rings stacked back to back, where GroES acts as a lid to the GroEL[59]. GroEL contains 14 subunits with each subunit at 57kDa, and GroES as a lid-like structure containing 7 subunits with a molecular weight of 10kDa [58]. Unfolded or misfolded protein substrates found within the cell are trapped within the hydrophobic interior of GroEL[60]. Upon ATP hydrolysis, the GroES traps the substrate within the hydrophobic interior[53]. The interior surface of GroEL facilitates protein folding when it converts from a hydrophobic to a hydrophilic surface [55, 61]. Studies have shown that GroEL exhibits little sensitivity towards oxidants such as nitric acid (NO) or hydrogen peroxide (H_2O_2) [60]. However, GroEL exhibited sensitivity and was inactivated when exposed to different oxidants such as hypochlorite (^-OCl) and peroxynitrite ($ONOO^-$)[60].

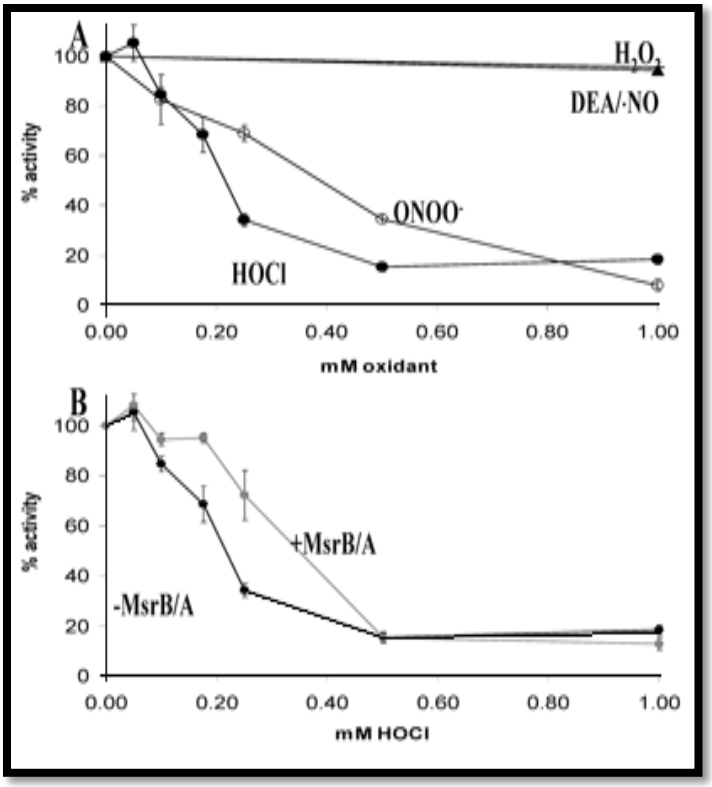

Figure 1.6. A) Comparing the GroEL activity as concentration of oxidant (HOCl & ONOO) increases; measured with reactivation of denatured malate dehydrogenase (MDH). B) GroEL samples were incubated with MsrB/A and compared the activity as HOCl concentration increases[60].

Figure 1.6.A. illustrates the activity of GroEL when refolding the denatured malate dehydrogenase (MDH) as the concentration of oxidants increases. MDH is a class III type substrate which requires GroEL/ES to refold[61]. Hydrogen peroxide and nitric acid shows no loss of activity of GroEL, however, when exposed to $^{-}$OCl and $ONOO^{-}$, more than half of its activity was lost [60]. The final concentration for this part of the experiment was as followed: 1uM native or oxidant-treated GroEL, 0.5uM MDH, 2uM GroES, and 5mM ATP [60]. The refolding reaction was carried out for one hour at 37°C [60]. In Figure 1.6.B, GroEL has been inactivated by HOCl. 1uM MsrB/A was added to the reaction and incubated with GroEL for two hours at 37°C, and was found to restore some GroEL activity [60]. Approximately 70, 85, and 60% of the activity lost was recovered after treatment of 0.1, 0.175, and 0.25mM HOCl,

respectively[60]. With the recovery of lost activity after the addition of MsrB/A to GroEL, this suggests that methionine is one of the amino acids responsible for protein inactivation [60]. A possibility of a complete reactivation of the denatured protein could be considered if the Met(S)O has been repaired to Met(O), as seen in Figure 1.7. After reactivation of the enzymatic function, further exposure of the unfolded protein with GroEL/ES will aid in regaining its native structure[24].

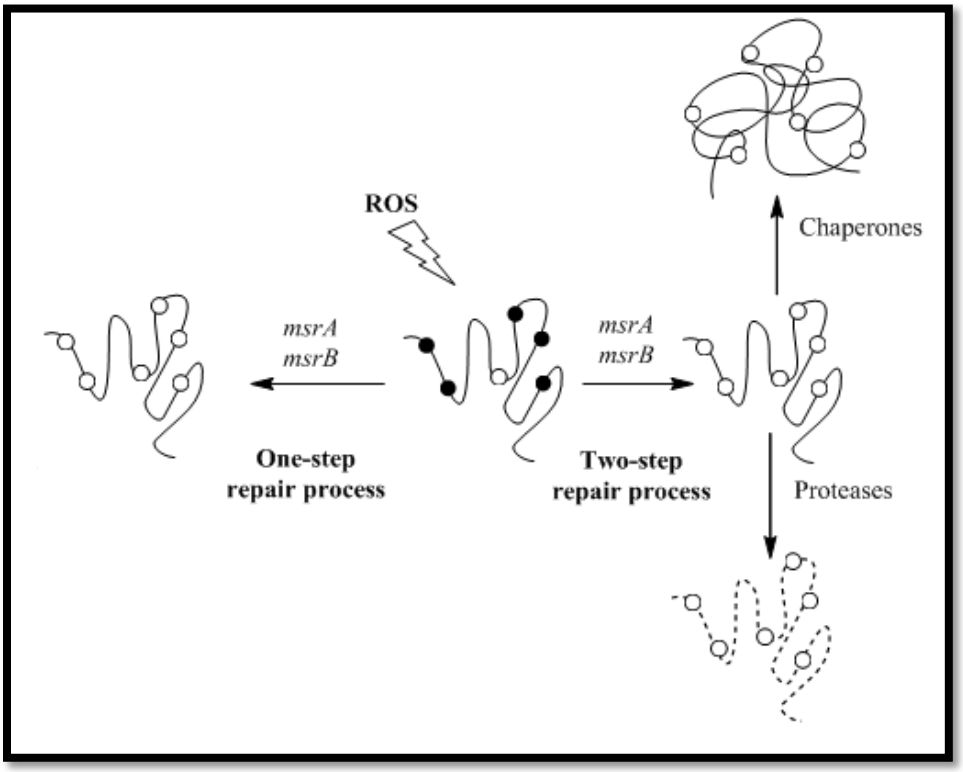

Figure 1.7. Possible pathways between protein oxido-reduction, folding and degradation pathways. Methionine residues are represented by the open circles while methionine sulfoxide represented by the black circles. The dashed line represents degradation while the dotted arrow represents a possibility of a direct link between an oxidized protein and the chaperones[24].

This thesis will present various experiments to quantify the oxidation and repairs targeted by Msr on certain methionine residues. A circular dichroism analysis was used to observe the catalase structure after different modifications, including varying molar excess of oxidants or treatment of GroEL/ES to verify the possibility of refolding an oxidized protein. Additionally,

samples were analyzed using a data dependant acquisition method on the Thermo Finnegan LTQ. However, due to low signal-to-noise ratio and non reproducible data, a different mass spectrometry technique, pseudo-MRM, was created. This technique produced more reliable data than the previous MS method.

CHAPTER 2

MATERIALS AND METHODS

Growth and isolation of *Helicobacter pylori* strain SS1

The Sydney strains (SS1) of *Helicobacter pylori* 26695 was used in this research as the parent strain[3]. Cultures were grown on blood agar at 37°C [3, 23]. Cloning was performed in *E. coli* strain DH5α, grown in Luria-Bertani medium supplemented with either ampicillin (100ug/mL) or kanamycin (25ug/mL) for selectivity [3, 23]. Plasmids used in this experiment for cloning include pGEM-T (Promega), pET21a (Novagen), and pBluescript KS(+) [3]. Growth was monitored by measuring the optical density at 600nm (OD_{600}) at each time point. Cells were disrupted by sonication (W-380 Heat System-Ultrasonics, Inc.) [23]. The collected cell lysate was then separated by 12.5% sodium dodecyl sulfate-polyacrylamide gel electrophoresis (SDS-PAGE), and immunoblotting was performed by use of anti-Msr antibody [23]. Cell extracts were centrifuged at 45,000 rpm for two hours to separate the soluble protein from the membrane protein pellet. The membrane fraction was suspended in 50mM Tris-HCl (pH 7.4) and stored in -80°C.

H. pylori methionine sulfoxide reductase (Msr)

The methionine sulfoxide reductase gene was inserted into the NdeI-XhoI restriction site of the plasmid pSAP112. The plasmid was then transformed into *E. coli* BL21 Origami (Novagen)[23]. *E. coli* strain harboring pSAP112 was incubated at 37°C until it achieved an OD_{600} of 0.6 [3, 23]. The culture was induced with 0.5mM isopropyl-β-D-thiogalactopyranoside (IPTG) at 22°C for 2.5 hours and the supernatant was loaded onto a Hi-Trap SP column (GE

Healthcare) [23]. Protein was then eluted using buffer B (50mM sodium phosphate and 1,000mM NaCl) with a linear gradient[23]. The fractions from the flow through were collected, applied to a HiTrap Q Sepharose column, and then eluted with the same buffers from above [3, 23]. The flow through fractions were then applied to a 10/200 Sephacryl column for size exclusion purification [23]. To assess the level of purification, the peak fractions were collected and subjected to SDS-PAGE [23].

Inactivation of *msr* in *H. pylori*

Mutants were obtained by insertional inactivation with an antibiotic cassette [3]. Starting with a 1500 base pair DNA fragment containing the msr gene, it was amplified by PCR using primers from genomic DNA of *Helicobacter pylori* 26695 and was cloned into plasmid, pGEM-T [3]. The selection marker used in the inactivation experiment is a kanamycin resistance gene *aph*A3 from *Campylobacter coli*, excised from plasmid pHP1 [62]. The Msr was inactivated by inserting a 1300 base pair blunt *aph*A3 fragment into the *Eco*RV site towards the 5'-end [3]. To inactivate only the msrB region, the *msr* was amplified using primers with a 400 base pair 3' flanking sequence and cloned[3]. The *aph*A3 was then inserted at the *Af*/II site towards the 3'-end[3]. The mutant strains were then obtained by allelic exchange of the *msr* with the plasmids containing the inactivated gene [3]. These mutant strains were also screened with PCR to confirm correct insertion of *aph*A3 [3].

Catalase purification from *H. pylori*

H. pylori cells were grown on blood agar plates for 40-44 hours. The colonies were then picked and washed with 20mM sodium phosphate – 150mM sodium chloride (pH 7.4). The cells were suspended in 25mM sodium phosphate – 50mM sodium chloride (pH 7.6) and lysed with three cycles of French press. The insoluble material was removed by centrifugation at 13000

rpm for 10 minutes and 45000 rpm for 45 minutes. The sample was then loaded onto the Hitrap SP column, which was pre-equilibrated with 25mM sodium phosphate – 50mM sodium chloride (buffer A). The samples were washed with buffer A and eluted with a linear gradient of 25mM sodium phosphate – 1000mM sodium chloride (pH 7.6). The catalase activity of the sample was checked in peak fractions. The peak fractions were then loaded on gel filtration and develop chromatogram in 20mM sodium phosphate – 150mM sodium chloride (pH 7.4). The pooled sample fractions were analyzed for any catalase activity as well as the purity of each fraction. The aliquots were prepared and stored at -80°C.

Isolation and purification of *H. pylori* GroEL/ES

GroEL/ES was purified from *Helicobacter pylori* strain SS1 [23]. The cells from blood agar was harvested in buffer A (50mM HEPES, 50mM NaCl, pH 7.2) followed by sonication where the cystolic fraction was subjected to ammonium sulfate precipitation [23]. At each purification step, GroEL/ES was monitored by *E. coli* anti-GroEL antibody (Sigma) [23]. The purified fractions of GroEL/ES were dialyzed overnight and then subjected to ion exchange chromatography using a HiTrap Q column [23]. The protein eluted from the column with a gradient of 50mM HEPES with an increasing range of 50mM NaCl to 1M NaCl [23]. The samples were separated by size exclusion using a 10/200 Sephacryl column equilibrated with 50mM HEPES (pH 7.4) with 300mM of NaCl. After all fractions have eluted off the Sephacryl column, the samples were then analyzed by SDS-PAGE [23].

Optimization of Digestion protocol for Data Dependant Acquisition

In order to obtain a digestion protocol to use for future experiments, catalase SS1 was obtained from Dr. Maier's group (Department of Microbiology, University of Georgia) which was expressed and purified from H. pylori. The digestion must be able to yield a reliable and a

high percent of sequence coverage of the 504 amino acid residues within its sequence. The fourteen methionine residues within catalase SS1 was also of importance for detection in the sequence coverage after digestion. The following are three different protocols that were used for optimization in data dependant acquisition.

The samples in the first protocol were dried down with a speed vacuum. The sample was resuspended in 10uL of 6M guanidinium hydrochloride (Gdmcl) with 50mM dithiothreitol (DTT) (pH 7.4) in order to reduce any disulfide bonds that are present. The catalase sample is then placed in heated water bath for an hour at 80°C to denature the protein. It was then diluted 10-fold in digestion with 20mM Ammonium Bicarbonate at room temperature. In order to analyze the protein sample, the addition of sequence grade trypsin (0.2ug/ul; Promega) was added into the sample to degrade the protein into polypeptides for quantification in the liquid chromatography-mass spectrometry.

The second protocol required the addition of 500mM of DTT into the catalase sample to reduce the disulfide bonds. This sample was also placed in a heat bath for an hour at 80°C for denaturation of the protein. The catalase was then removed from the water bath and cooled down to room temperature. Equal amounts of ammonium bicarbonate were added to the sample. Following the addition of ammonium bicarbonate, 1uL of 0.02ug/ul trypsin (Promega) was added to the sample for digestion.

A combination of 6M gdmcl and 100mM DTT were added to the catalase sample in the last protocol. The samples were then placed into the water bath for an hour at 80°C. Following the heat denaturation of catalase, the samples were diluted with a 5-fold molar excess of ammonium bicarbonate. The samples were then partially dried by a speed vacuum until the total volume is equivalent to the other samples from the previous two protocols. The denatured

samples were digested into peptides with the addition of sequence grade modified trypsin (0.2ug/ul; Promega). All samples were then placed into a hybridization oven at 37°C for 24 hours. After exposure to the digestive enzyme overnight, the samples were then packed onto nanofrit columns used with liquid chromatography methods.

Digestion Protocols for Pseudo-MRM

Sequencing grade modified trypsin (Promega) is a serine protease used as a digestive enzyme to hydrolyze the peptide bonds at the c-terminal of lysine and arginine residues, except when followed by a proline residue. The trypsin from Promega has been modified by reductive methylation which prevents autolytic digestion. Autolytic digestion involves the generation of fragments that interferes with protein sequencing and analysis of peptides by mass spectrometry. The catalase samples were diluted to the same concentration (200ug/uL). Approximately 2ug of catalase proteins were divided into aliquots. 1uL of a 50mM DTT-500mM ammonium bicarbonate (pH 7.8) was added into each aliquot to reduce any disulfide bonds present in the protein. The samples were then heated in a water bath for thirty minutes at 90°C for denaturation of the catalase. The samples were removed from the water bath and set to cool to room temperature for ten minutes. Sequence grade modified trypsin was diluted to 0.2ug/uL and the calculated amounts of trypsin were added for each sample. The samples were incubated overnight for 24 hours at 37°C.

Endoproteinase aspartic-N (asp-N) (Sigma) is a metallo enzyme used alone or in combination with other proteases to produce protein digests for peptide mapping or protein identifications by mass spectrometry. Asp-N hydrolyzes peptide bonds on the N-terminal side of aspartic acid. Another digestive enzyme was used to obtain a higher combined total sequence coverage from both trypsin and asp-N digestion. This was achieved by the different cleavage

sites of asp-N enzyme which resulted in detection of methionine residues which were not detectable with the trypsin digest. The protocol for the catalase digestion required 2.5ug of protein in ammonium bicarbonate buffer (pH 7.4) with 1mM DTT to hydrolyze any disulfide bonds. The samples were heat denatured for five minutes at 95°C and then cooled off to room temperature. Aliquots of 0.025ug of asp-N were added two times at a total of 0.05ug at a ratio of 1:50 to catalase. The first aliquot of asp-N was added and incubated at 37°C for three hours. The second aliquot of asp-N was added into the samples and further incubated for two hours for a total of five hours of incubation at 37°C.

Nanofrit column packing

In order to pack a nanofrit column for use in mass spectrometry, the silica capillary (363 OD, 79 ID, 19.5 tube coat) was cut at 22 cm. It was then fluxed into two columns. First, the capillary was loaded with a C18 saturated solution (in 50/50 isoproponal (IPA)/methanol (MeOH)) until it is visibly seen as packed for approximately 7-8cm from the bottom of the column. The column was then washed with 50/50 IPA/MeOH for 30 minutes. After the initial wash, the column was subjected to MeOH for 30 minutes followed with 80% acetonitrile for another 30 minutes and then 0.1% formic acid for 30 minutes. A standard sample was loaded onto the packed column for 30 minutes under high pressure. The standard was then tested on the LC-MS/MS with a data dependant acquisition method for the elution of the standard off the column. Once the standard has met the correct requirements, the column was then washed with the earlier procedures and loaded with the samples for 45-50 minutes before loading it back onto the LTQ.

Converting RAW files to .pkl files

After all runs have been completed, the RAW files were then transferred to another storage site where it will be analyzed. The RAW file was then converted into a file type (.pkl) which was recognizable by MASCOT, a search engine that uses mass spectrometry data to identify proteins from primary sequence databases. In order for a RAW file to be converted to a .pkl file it must first be converted to mzxml, which was accomplished by using a perl script. A linux operated program, SSH secure, converted the new mzxml files to pkl and for use in MASCOT.

Circular Dichroism protocol

Circular Dichroism analysis was performed on a JASCO spectropolarimeter (Easton, MD). *H. pylori* catalase was purified and isolated as mentioned with the earlier steps. The samples were then treated with excess HOCl and quenched with excess methionine. Two different experiments were carried out with circular dichroism to observe any structural changes to catalase under different modifications. The first set of samples was treated with varying molar excess (0, 30, 60, and 100) of hypochlorous acid (HOCl) for 15 minutes. The final experiment involved the comparison of an unoxidized catalase, oxidized catalase with 60-fold molar excess HOCl, and the oxidized catalase treated with GroEL/ES for possible refolding of the structure [23]. Far-UV spectra were recorded at room temperature from 190-250 nm with a 0.1mm path-length cell. All catalase samples were analyzed at concentration of 200ug/mL in sodium phosphate buffer (20mM, pH 7.4).

MS Data Dependant Acquisition Protocol

The samples were purified and isolated as previously described. Catalase was then subjected to excess HOCl and quenched with excess methionine. In this set of data dependant

acquisition experiments, interaction with catalase *in vivo* and *in vitro* was studied. *In vitro* studies observe the role Msr has on either unoxidized catalase or oxidized catalase. In contrast to the *in vitro* studies, *in vivo* studies concentrated on the roles mutant strains versus the wild type strains of Msr. All samples were then reduced with DTT to break the disulfide bonds. Denaturation of the samples was accomplished with a heated water bath at 80°C for an hour. Following the denaturation process, sequence grade trypsin was added to the sample for digestion of proteins into polypeptides. The samples were then placed in a heated water bath for protein denaturation. Aliquots of 1uL of sequence grade trypsin (0.4ug/uL) were treated with catalase samples for digestion of the proteins. The loaded nanofrit column was attached to a split flow coming from an Agilent HPLC. A gradient from 5% - 60% acetonitrile runs over the column over a period of 70 minutes, followed by a steep gradient from 60%-95% acetonitrile over 10 minutes to wash the column. All solvents use 0.1% formic acid as an acidifying agent and weak ion pairing reagent. Mass spectrometry was performed using a 7T LTQ-FT hybrid mass spectrometer. MS scans were performed by FT-ICR MS, with a nominal resolution of 50k at m/z 1000. Up to 9 concurrent MS/MS experiments were performed in the linear ion trap during each FT-ICR scan in a data-dependant fashion, with each precursor fragmented up to 4 times in any 5 minute window to prevent oversampling of abundant precursors. Precursor ions were fragmented by collision-induced dissociation, with a normalized collision potential of 35V, an activation time of 30ms, and a standard activation Q of 0.250.

The raw data were then analyzed and searched on MASCOT for sequence coverage and reproducibility. The raw data was also analyzed by manually searching for the precursor ions of the peptides which includes a methionine residue. The fraction oxidized was calculated by

comparing the area of the oxidized peak over the sum of the area of the oxidized peak with the area of the unoxidized peak.

MS Pseudo-MRM

Pseudo-MRM was introduced when using data dependant acquisition method was not producing reproducible data. The catalase was grown on blood agar, isolated, and purified with multidimensional chromatography. The samples were treated with excess molar excess concentration of HOCl and later quenched with excess methionine. For this technique, the sample was treated with different oxidants and Msr. All samples were reduced with DTT to break disulfide bonds. The samples were placed in a heated water bath to denature the protein and treated with either sequence grade trypsin or Asp-N for digestion of the proteins into polypeptides.

From the data dependant acquisition technique, a list of precursor and product ions was extracted from the MS data. The precursor ions were entered onto an include list during method development on the Finnegan LTQ program software. This will program the LTQ to continue scanning until it detects a precursor ion where the LTQ will isolate the ion and scan it for MS/MS with a minimum signal threshold of 500 counts. The normalized collision energy was set at 35V. Analyzing the data includes the addition of the product ion (related to the specific precursor ion) into the XCalibur analytical software. Just as the data dependant acquisition, the fraction oxidized was calculated for each methionine residues.

Mass spectrometry was performed using the Thermo Finnegan LTQ coupled with the Agilent LC. MS scans were performed by the LTQ scanning up to 9 concurrent MS/MS experiments in a data dependant fashion. The precursor ions were fragmented by collision-induced dissociation with a normalized collision potential of 35V, an activation time of 30ms,

and a standard activation Q of 0.250. From the data dependant acquisition method, the precursor and product ions were extracted from the MS data. The precursor ions were entered onto an include list during method development as part of the Thermo Finnegan LTQ software program. The LTQ scans until a listed precursor ion was detected which was further isolated and fragmented. The fragmented ions were ejected into the detector and scanned for MS/MS at a minimum signal threshold of 500 counts. The raw files were then manually analyzed by isolating the precursor ion and product ion in the analytical software, Xcalibur V1.4. To analyze for the percent of oxidation for specific methionine residue, the area of the oxidized peak in a base peak chromatogram was divided by the total area of the oxidized and unoxidized peaks.

CHATPER 3

CIRCULAR DICHROISM ANALYSIS

Oxidative stress causes damages to amino acid residues leading to the loss of native enzymatic activity. Structural effects of oxidized catalase were of particular interest and were examined with circular dichroism. Circular dichroism (CD) spectroscopy analyzes chiral macromolecules by measuring the difference between the absorption of polarized light either dextrorotatory or levorotatory over a range of wavelengths. The primary use of CD is used to identify secondary structure of a macromolecule such as alpha helix, beta sheets, and random coils (Figure 3.1). Measurements are studied in the visible and ultra-violet region and used to predict the percentages of the secondary structure in the protein. If the protein contains any chiral chromophores, then one of the circular polarized lights will be absorbed more than the other. The CD will record the ellipticity of the protein at a specific wavelength. CD can be utilized for many other studies such as protein-protein or protein-ligand interactions, or the effects of how the environment can change the structural conformation of the protein.

CD was used as a qualitative method to study the catalase structure when modified either by oxidants or chaperonins. The first experiment will focus on the structural effects oxidation has on catalase by increasing the molar excess of HOCl. As a cell loses its enzymatic function with the increase of oxidative stress, the increasing amounts of HOCl will also cause the catalase to lose its structure. As mentioned in the introduction, GroEL/ES is a chaperonin known to facilitate refolding of proteins. The following experiment will test and analyze the role GroEL/ES treatment to an oxidized catalase. The treatment of GroEL/ES should refold and

restore the activity of the oxidized catalase. Protocols for these experiments are found in Chapter 2: Circular Dichroism protocol. To briefly reiterate the protocol, the samples were grown on blood agar, isolated, and purified by chromatography. The catalase was then treated with excess HOCl and quenched with excess methionine. Depending on the experiment, the samples were either treated with different dosages of oxidants or treated with GroEL/ES. The samples were then placed into a cuvette and scanned on the CD spectropolarimeter to yield a spectrum.

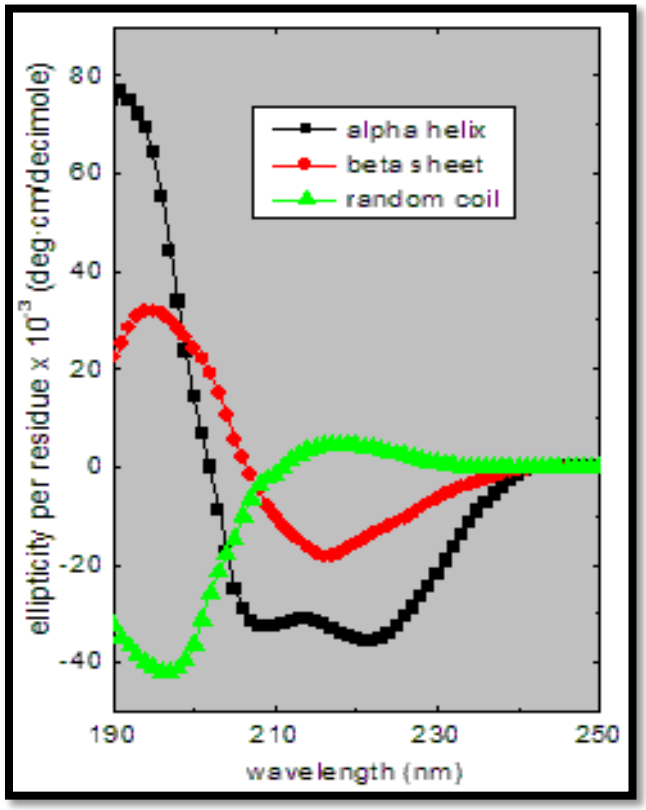

Figure 3.1. A typical CD spectrum including characteristics shapes of alpha helix, beta sheet, and random coil.

Results

The first set of experiments included catalase samples with varying molar excess of HOCl (0, 30, 60, and 100). As seen in Figure 3.2, CD analysis of the different samples exhibited a difference in structure as the concentration of HOCl increases. The unoxidized catalase resulted in a deconvoluted spectrum with a predicted secondary structure composition of 29%

alpha helix, 21% beta sheet, with an expected maximum error of 8%. This result was in agreement with the published X-ray crystal structure (PSB ID 2IQF), which had 32% helix and 18% beta sheet. Upon oxidation at 30x molar excess HOCl, an overall loss of dichroism is noted. Deconvolution of the 30x molar excess HOCl-oxidized catalase reveals a 30% alpha helix, 13% beta sheet; a marked decrease in the beta sheet content. Upon 60x and 100x molar excess HOCl-oxidized catalase, the CD spectrum illustrated the loss of structure as the oxidation level increased.

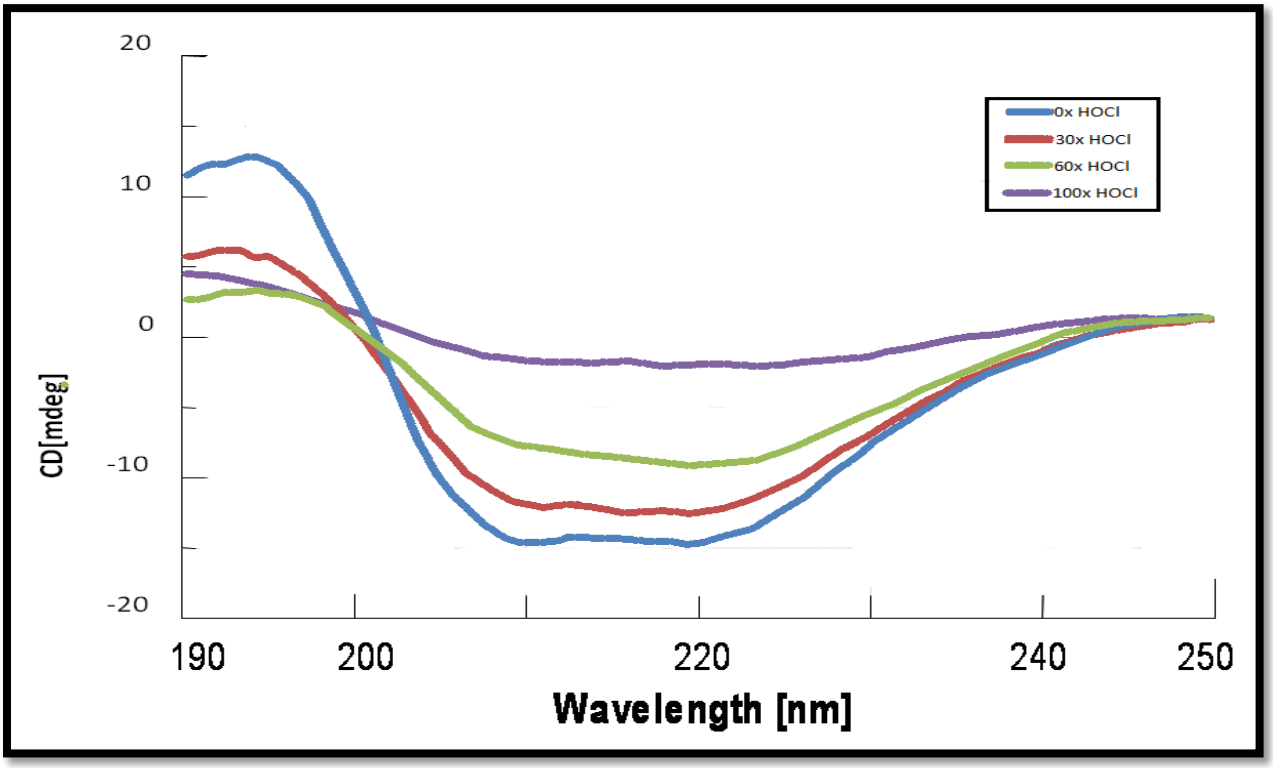

Figure 3.2. CD analysis of the unoxidized catalase (blue) compared to different levels of oxidation: 30x (red), 60x (green), and 100x (purple).

The CD spectrum exhibited in Figure 3.3 includes an unoxidized catalase sample (blue), an oxidized catalase with 60x molar excess of HOCl (red), and a sample with the introduction of GroEL to an oxidized catalase (green). The unoxidized catalase was depicted with the expected amounts of alpha helix and beta sheets, similar to Figure 3.2. However, once oxidized with HOCl, the structure of catalase loses some of its alpha helix and beta sheets structure. The

treatment with GroEL should refold the oxidized catalase to its native form as well as catalase activity being restored. Compared to the HOCl sample, the addition of GroEL to the sample seemed to have an increase in both alpha helix and beta sheets; evidence of partial repair to the oxidized sample. In this figure, the GroEL sample was compared to the weighted mean average of the 48% catalase and 52% oxidized catalase as a representation of GroEL partially repairing an oxidized catalase. The reduction of catalase with Msr followed by the treatment of GroEL was also subjected to CD experimentations. However, data were not reproducible due to errors in sample preparations.

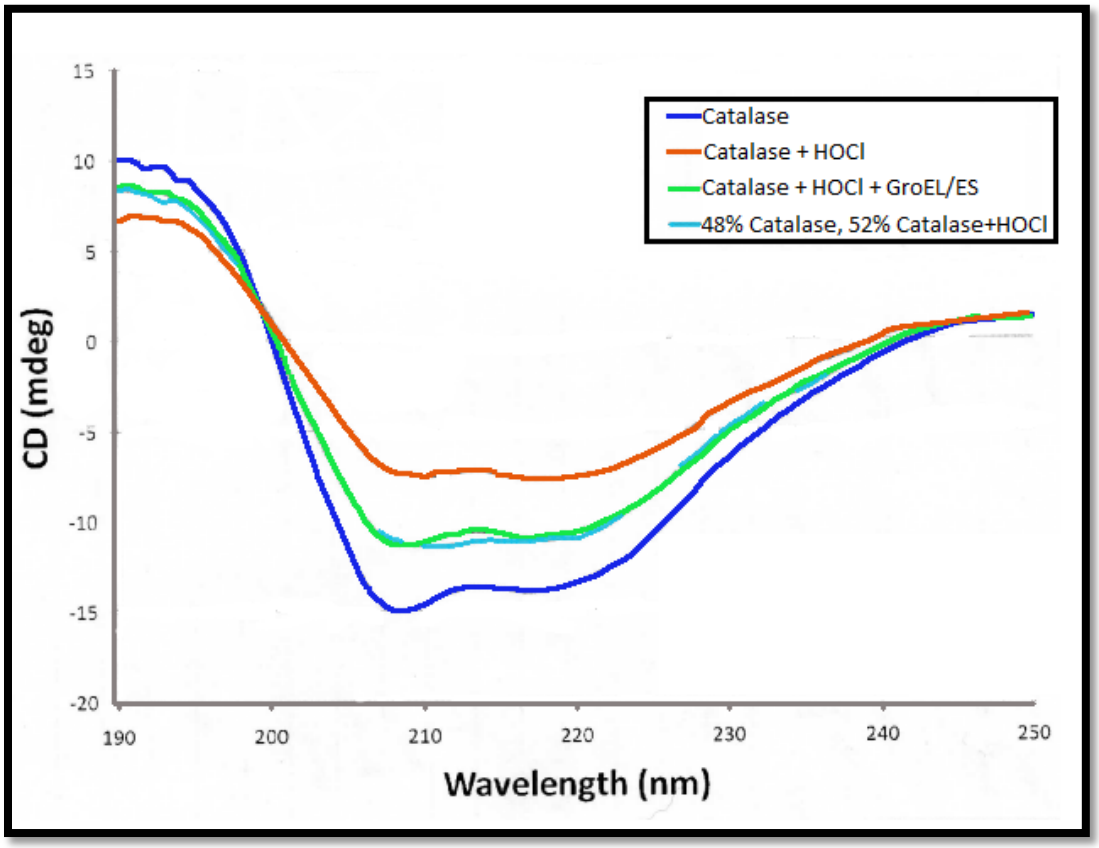

Figure 3.3. Circular Dichroism spectrum including catalase (blue), oxidized catalase with 60x molar excess HOCl (red), oxidized catalase treated with GroEL/ES (green), and weighted average of unoxidized and oxidized catalase (light blue).

Conclusion

Circular dichroism reflects the secondary structures of macromolecules such as alpha helix, beta sheets, and random coils. Samples from different experiments were analyzed on the spectropolarimeter for detection of any structural changes. As exhibited in Figure 3.2, CD scans confirmed that the secondary structure of catalase unfolds as the oxidants increased. These results were compared with the catalase activity (Figure 3.4) obtained from the Maier's group comparing effects of catalase as oxidants increased. The activity of catalase was decreased as the molar excess of HOCl increased. These experiments confirmed the decreased in catalase activity correlated to the loss of secondary structures of oxidized catalase.

GroEL/ES is a chaperonin known to facilitate in refolding proteins. To qualitatively analyze the role of GroEL/ES, CD was used to observe structural changes before and after treatment of GroEL (Figure 3.3). CD scans confirmed GroEL/ES and the role of facilitating protein refolding as GroEL/ES regained some of its lost structure when treated to oxidized catalase. The results from CD scans were compared to the catalase activity obtained from the Maier's group seen in Figure 3.5. As seen in both 30x and 60x molar excess HOCl, the native catalase exhibits 100% catalase activity. However, the activity of oxidized catalase significantly decreased. Treatment of GroEL to the damaged catalase increased catalase activity and interestingly was more effective in restoring activity than Msr. The role of GroEL treatments to oxidized catalase partially restored the structure as well as the catalase activity. Not only did Figure 3.5 exhibited the increased of catalase activity with Msr and GroEL, it also stated that a combination of both repairing and refolding treatments to an oxidized catalase will increase the catalase activity greater than the treatments as separate reactions. A CD experiment was applied to the combination of Msr and GroEL; however, CD scans did not correlate to the catalase

activity figure. A possible reason for this problem was caused by samples preparations. The combination of Msr and GroEL to an oxidized catalase will be retested again in the future.

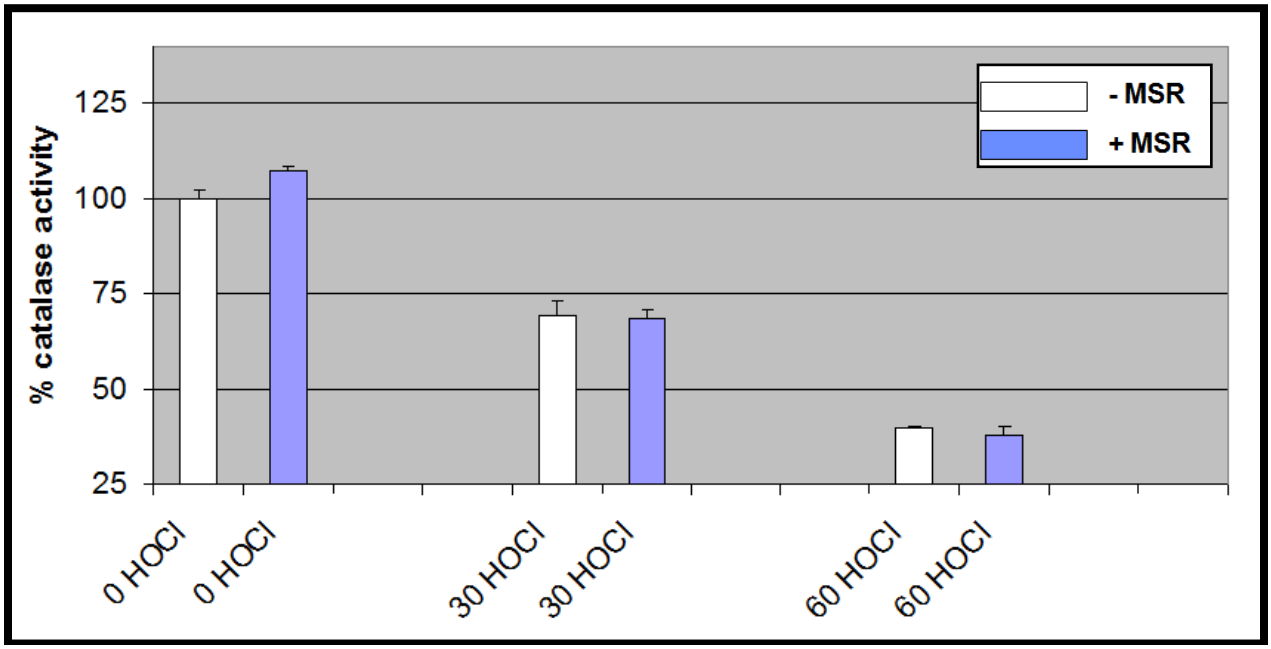

Figure 3.4. Catalase activity of oxidized catalase with increasing molar excess of HOCl comparing catalase with (blue) and without (white) treatment of Msr

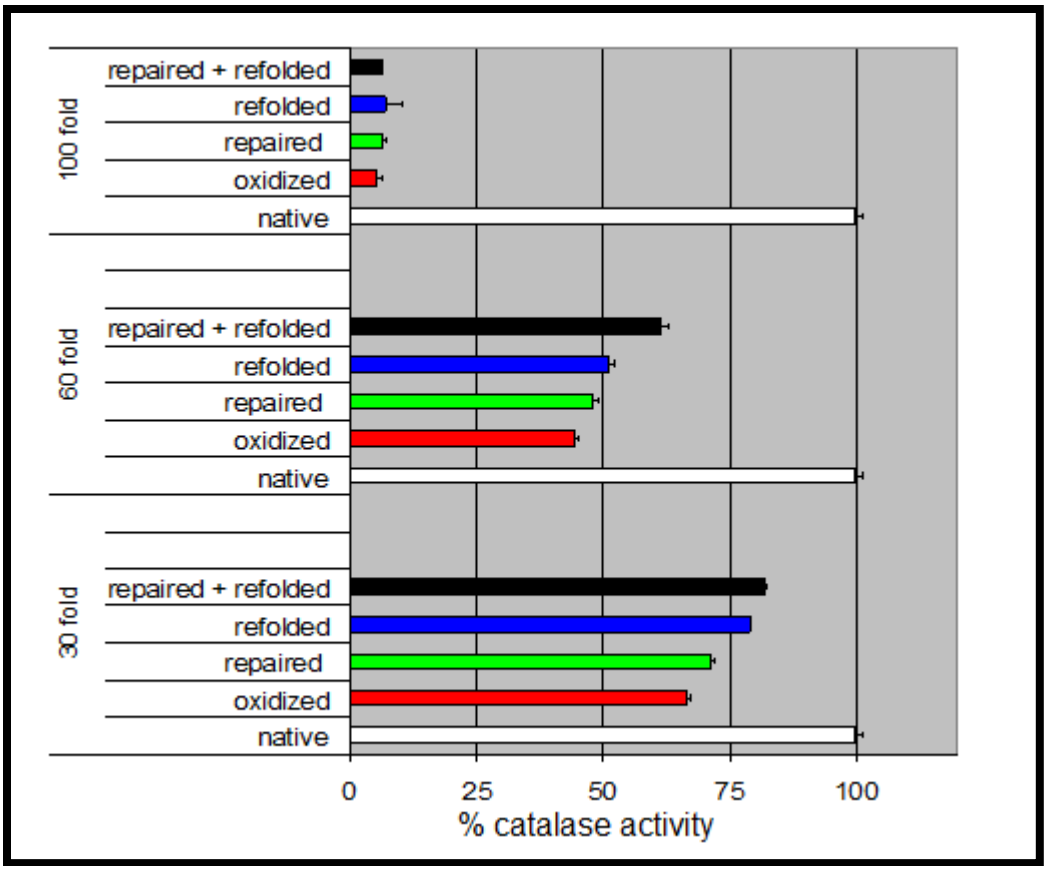

Figure 3.5. Msr and GroEL synergistically repairs HOCl damaged catalase. Unoxidized catalase (white), oxidized catalase (red), oxidized catalase treated with Msr (green), oxidized catalase treated with GroEL (blue), and oxidized catalase treated with both Msr and GroEL (black) are compared by the percent catalase activity.

CHAPTER 4

MS DATA DEPENDANT ACQUISITION

This chapter will discuss the *in vivo* and *in vitro* samples submitted to the data dependant acquisition method. As described in Chapter 2, samples were isolated and purified with chromatography. Catalase was then treated with excess molar concentration of HOCl and then quenched with excess methionine. The samples were then subjected to a trypsin digest and loaded onto a nanofrit column. Data dependant acquisition was performed on an Agilent LC coupled with a Thermo Finnegan LTQ. LTQ (linear trap quadrupole) comprises of an ion trap where the ions can be trapped, isolated, and ejected into the detector for MS or MS/MS scans. For data dependant acquisition, the ions are first collected in the ion trap and scanned for the top nine precursor ions and ejected into the detector. These precursor ions were then isolated and then further fragmented into product ions. The product ions were later ejected into the detector yielding MS/MS data. Data dependant acquisition of an unknown sample provided data with retention times along with the precursor and product ions of specific peptide sequences. Data collected were analyzed by Mascot against a database consisting solely of the catalase sequence provided by the Maier lab, with dynamic oxidations of methionine to methionine sulfoxide enabled. The MS/MS data was also analyzed manually at each peptide sequence containing the targeted methionine residue to quantify the percent of oxidation.

Treatment of Msr on catalase *in vitro*

In vitro experiments were done in laboratory vessels such as Petri dishes and test tubes in a controlled experimental environment. The following samples consists of different

combinations of Msr and catalase used for *in vitro* experiments: unoxidized catalase with no Msr, unoxidized catalase with Msr, oxidized catalase with no Msr, and oxidized catalase with Msr. For each combination, observation of the sequence coverage and amount of oxidation calculated for each methionine will be discussed. Base peak chromatogram at a specific m/z corresponds to a peptide sequence containing a methionine residue (Figure 4.1). To confirm that the peaks correspond to the correct peptide, the sums of the peaks are depicted in the MS/MS spectra in Figure 4.2. Once the MS/MS spectrum has correctly identified the peptide fragment ions to the corresponding methionine residue, the area found in the base peak chromatogram were later used to calculate the percent oxidation per methionine residues. An example of the calculation can be seen in Equation 4.1, in which the area of the oxidized peak was divided by the total of the area of the oxidized peak and unoxidized peak yielding the fraction oxidized of methionine residue.

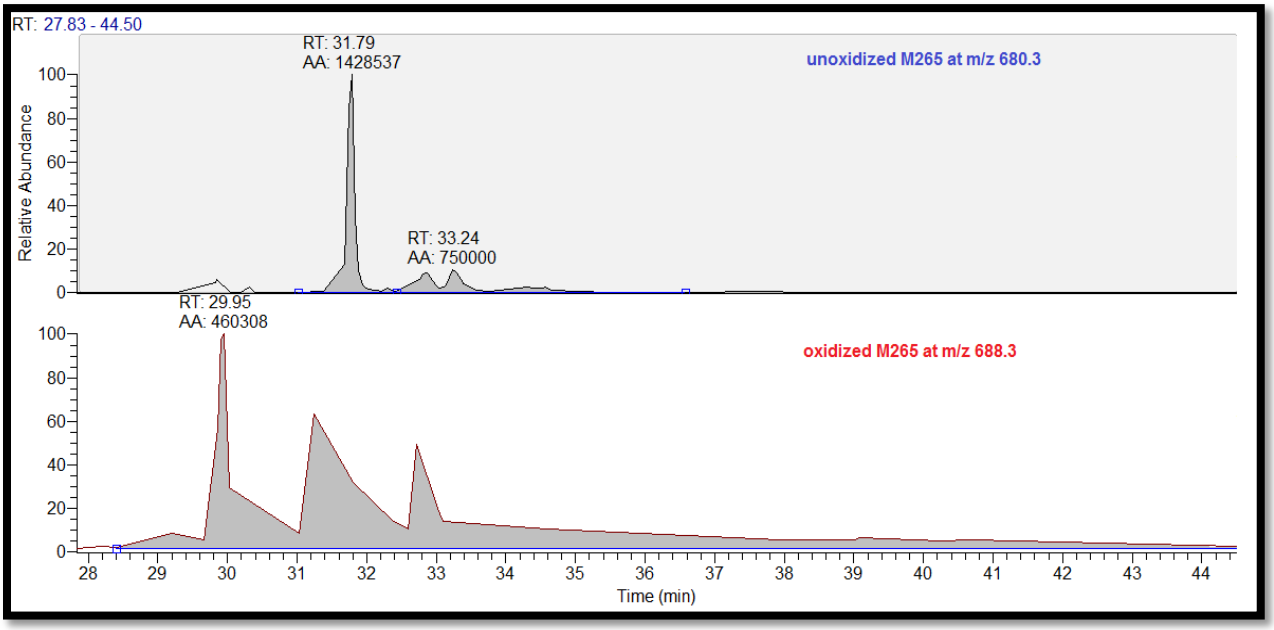

Figure 4.1. Base peak chromatogram of M265. The top chromatogram is the unoxidized M265 at the m/z of 680.3 while the bottom chromatogram represents the oxidized M265 at m/z 688.3.

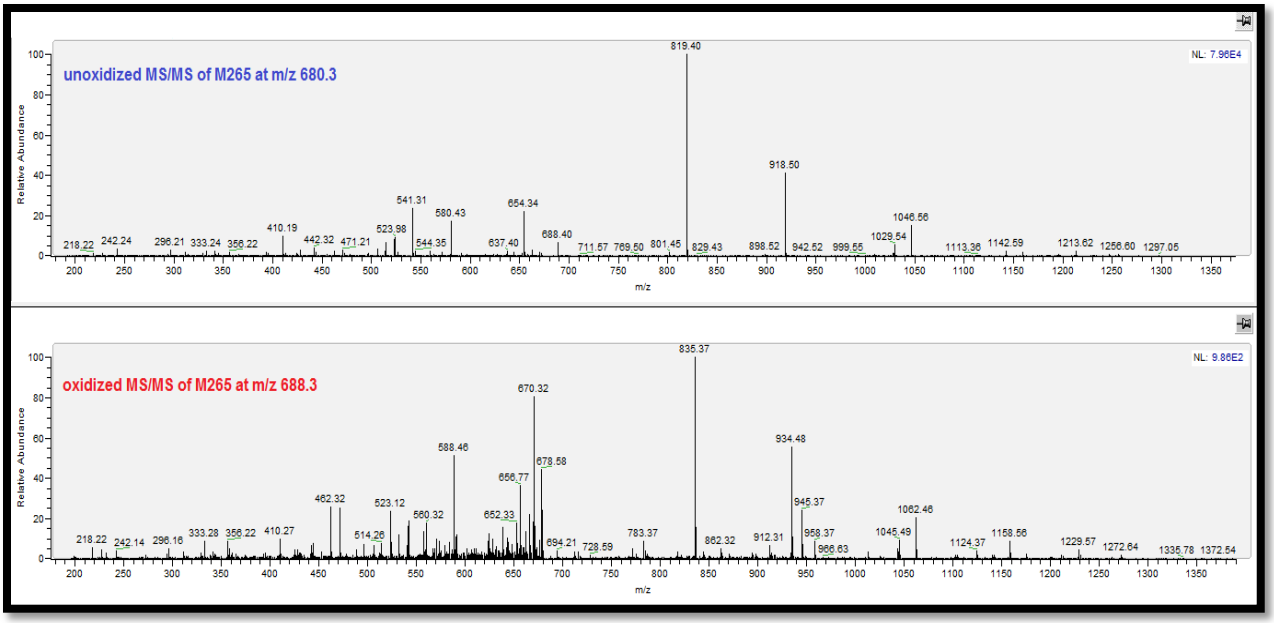

Figure 4.2. MS/MS spectra of unoxidized and oxidized M265. The top MS/MS spectrum shows unoxidized M265 at m/z 680.3 while the bottom represents the oxidized MS/MS spectrum of M265 at m/z 688.3.

$$\frac{oxidized}{oxidized + unoxidized} = \frac{460308}{460308 + 1428537} = 0.24 \quad \text{(Equation 4.1)}$$

MS/MS of an untreated catalase achieved a maximum of 72% sequence coverage with 6 of the 14 methionines detected (Figure 4.3). The missing methionines can be found in the C-terminal of the protein. Of the 6 detected methionines, three were detected as oxidized methionines: M1, M265, and M372. M1 was found to be ~27% oxidized. M265 was found in two partial digestion products with ~36.1% oxidation and ~36.4% oxidation. Approximately 8.9% of M372 was oxidized. The other methionines (M162, M181, and M292) that were found in the database search were not detected as oxidized by mass spectrometry to a significant extent.

Figure 4.3. Sequence coverage of the unoxidized catalase sample with no Msr. 72.4% (bolded red) was recovered from the sequence with 6 methionines detected. Out of the 6 methionines detected (unoxidized: blue), only three were found to be oxidized (green).

The next set of samples was analyzed to detect the effects of Msr on an unoxidized catalase. As seen in Figure 4.4, MS/MS achieved a maximum of 68.85% sequence coverage with 8 of 14 methionines detected. The noticeable change between the unoxidized catalase with treatment of msr to the control is the identification of partial digestion products containing three methionines near the C-terminus. Another difference can be found in that the peptide containing M162 was not identified in this sample. Of the eight methionines, three were identified as oxidized (M1, M265, and M372). M1 was oxidized ~16.5% while M265 had partial digestion with the most intense oxidation product at 12.3% while the other partial digestion at 27%. M372 was oxidized to 26%. The other five methionines (M292, M331, M488, M489, M492) identified were not identified as oxidized by MS/MS.

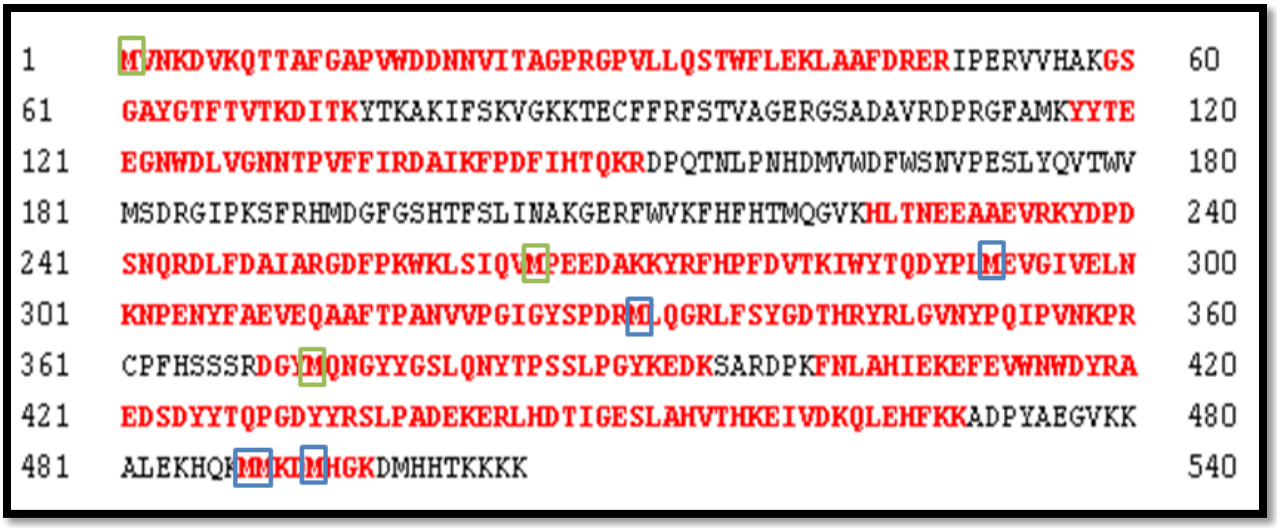

Figure 4.4. Unoxidized catalase with the addition of Msr. Catalase was observed with a 68.85% sequence coverage (bold red) and eight out of fourteen methionine detected. Similar to Figure 3.1, three methionines were calculated to be oxidized (green) while the rest were unoxidized (blue).

The following set of catalase samples were oxidized with no addition of Msr (Figure 4.5). According to the MS/MS data, there was maximum sequence coverage by MS/MS of 88.2% with 10 out of 14 methionines detected. Of these 10 methionines, only six were identified as being oxidized: M115, M162, M220, M265, M292, and M372. While M1 was not detected as oxidized by MS/MS, the oxidized peptide was detected by mass and relative retention time in the MS scan and can be quantified with a 58.2% oxidation. M115 was oxidized to 26.4% while M162 was only detected as being oxidized with very low oxidation percentages. M193 was only detected as unoxidized. M220 was 81.1% oxidized. M265 was again detected in multiple peptides with different amounts of oxidation. The complete digestion product had 13.8% oxidation. The same region with one missed cleavage was detected with 6.8% oxidation while the last one with 2 missed cleavages was 2.7% oxidized. M292 was 88.3% oxidized. M331 was detected only as unoxidized by MS/MS but the oxidized peptide could be measured in the MS scans and quantified as 9.9% oxidized. M372 was 80.6% oxidized.

Figure 4.5. Oxidized catalase with no Msr present. Sequence coverage (bold red) of 88.2% was observed with 10 methionines detected. Six methionines (green) were calculated as oxidized while the remaining methionines (blue) are observed as unoxidized.

The samples containing the oxidized catalase with Msr treatment was analyzed to detect any repair of oxidized catalase with the reductase (Figure 4.6). The maximum sequence coverage by MS/MS for this particular sample set was 83.5% with 8 out of 14 methionine detected. The difference between this sample and the oxidized catalase without treatment was the lack of two small peptides in the middle of the sequence containing M115 and M220. However, one of these peptides was detected by mass at the appropriate point in the chromatogram and can generate quantitative measurements of oxidation. The quantitative measurements were not obtained from the MS/MS spectrum. M1 was detected by MS/MS only in the unoxidized form but the oxidized version could only be seen by MS with a 67.2% oxidation. M115 was not detected in any form by MS/MS but the peptide mass was found in the MS with an oxidation of 18.4%. M162 was 38% oxidized. M193 was only detected as unoxidized. Three peptides with M265 were again detected, ranging from 1.7% oxidized for two missed cleaves to 12% oxidized for the complete digestion product. M292 was only detected in the oxidized form. M331 was detected only as unoxidized by MS/MS however was seen by MS scans with a 32.5% oxidation. The last methionine, M372, was 37% oxidized.

Figure 4.6. Oxidized catalase with the addition of Msr. The maximum sequence coverage (bold red) was observed at 83.5% with 8 methionines detected. 4 methionines (green) were observed as completely oxidized in the MS/MS scans, while the other methionines (blue) were found as unoxidized.

Table 4.1. Oxidation of *In Vitro* samples. Highlighted in red, the percent oxidation of selected methionine residues exhibited a decrease in oxidation when Msr was added.

Methionine	Sample	[oxidized]/[total]	Standard Dev
265	+HOCl +Msr	0.144	0.016
	+HOCl –Msr	0.209	0.040
	-HOCl +Msr	0.059	0.006
	-HOCl –Msr	0.082	0.014
115	+HOCl +Msr	0.247	0.004
	+HOCl –Msr	0.492	0.116
	-HOCl +Msr	0	0
	-HOCl –Msr	0	0
372	+HOCl +Msr	0.261	0.069
	+HOCl –Msr	0.243	0.078
	-HOCl +Msr	0.167	0.085
	-HOCl –Msr	0.191	0.035
497	+HOCl +Msr	0.545	0.121
	+HOCl –Msr	0.707	0.104
	-HOCl +Msr	ND	ND
	-HOCl –Msr	ND	ND
331	+HOCl +Msr	0.208	0.086
	+HOCl –Msr	0.245	0.088
	-HOCl +Msr	ND	ND
	-HOCl –Msr	ND	ND

Comparison of Wild type vs. mutant type strains *in vivo*

Experiments performed *in vivo* were completed to analyze the difference of oxidation between the wild type strains of Msr (which can be found in the body) versus the mutant *msr* strain (genetically inactivated with an antibiotic cassette). The major difference between the *in vitro* studies compared to the *in vivo* studies was based on when the catalase was extracted from the sample. The catalase was already purified and extracted from the beginning of the protocol. However, the catalase in the *in vivo* studies was extracted after treatments of both oxidants and Msr. As previously tested in other labs, the mutant *msr* strain exhibited high susceptibility towards oxidants. The following samples were analyzed by comparing the treatment of different oxidants on wild type strain (Msr) against the msr mutant (*msr*): Msr strain with PBS buffer, Msr strain oxidized with hydrogen peroxide, Msr strain oxidized with hypochlorite, *msr* strain with PBS buffer, *msr* strain oxidized with hydrogen peroxide, and *msr* strain oxidized with hypochlorite. Both strains of methionine sulfoxide reductase were subjected to different oxidants to detect if there were any differences in oxidation level and intensity as it appears on the LTQ.

Results:

Wild type strain (Msr) with PBS has maximum sequence coverage of 47.2% with 5 of 14 methionines found as seen in Figure 4.7. M115 was detected at 29.2% oxidation. M265 was partially digested into two peptides with oxidation of 14.9% and 12.9%. M331 was detected at 11.2% oxidation. Two residues (M492 and M497) from the C-terminus were detected with an oxidation of 42.7%.

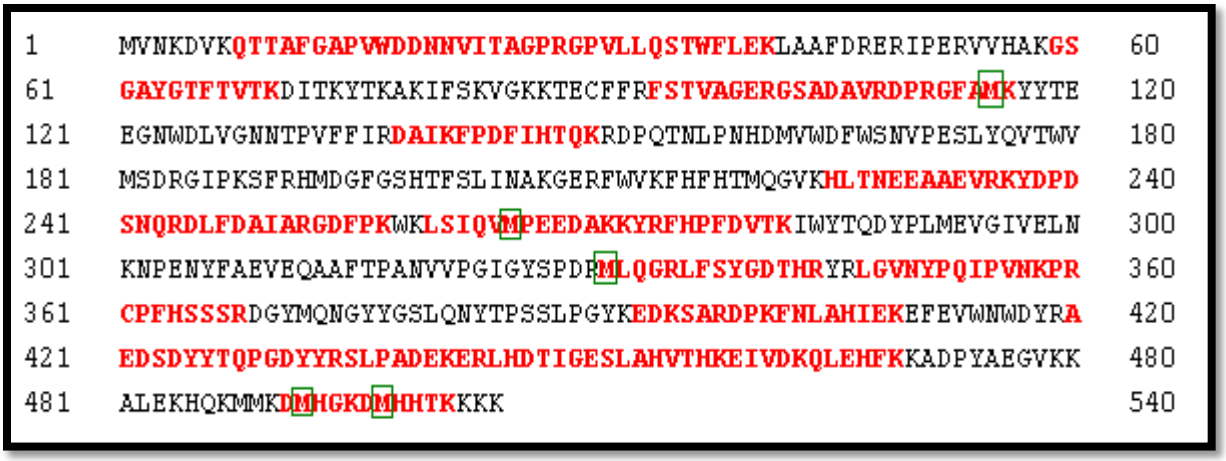

Figure 4.7. WT Msr with PBS with sequence coverage (bold red) of 47.2%. Three oxidized (green) and two unoxidized (blue) methionine were detected.

Shown in Figure 4.8, wild type strain Msr with HOCl has sequence coverage of 39.5% with 5 out of 14 methionines detected. None of the methionines from the N-terminus was detected. M193 was detected with an oxidation of 19.2%. M265 was partially digested into two peptides with oxidation of 19.3% and 18.3%. M331 was found with an oxidation of 15.1%. M372 was detected at 63.9% oxidation. Two residues (M492 and M497) from the C-terminal were detected at 20.1%.

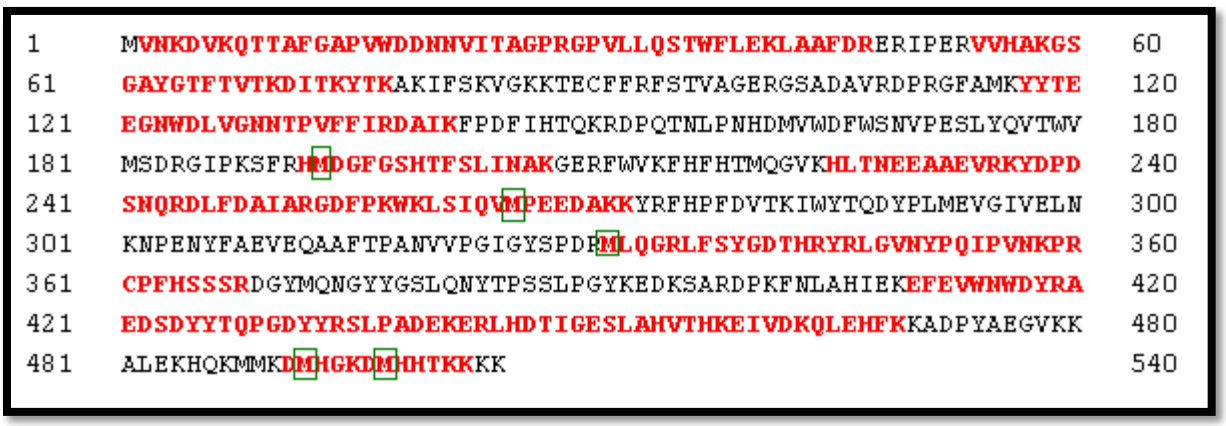

Figure 4.8. Msr oxidized with HOCl with observed 39.5% sequence coverage (red). All 5 methionines were detected as oxidized (green).

Wild type strain Msr with H_2O_2 was detected with maximum sequence coverage of 74.4% with all methionines being detected (Figure 4.9). Only 13 of the 14 were actually detected as oxidized. M1 was found at 45.2% oxidation. M115 has approximately 15.2% oxidation. M162 and M181 are from the same peptide sequence with an oxidation of 51.2%. The trypsin digest were not able to separate the two methionine residues into separate peptides thus M162 and M181 are calculated as one long peptide. M193 was oxidized at 54.5%. At M220, oxidation was detected with a 44.7% oxidation. At M256, the peptide sequence was partially digested into two sequence and both have an oxidation of 51.2%. M193 has an oxidation of 54.4%. M292 was detected with an oxidation percent of 31.5% and approximately 32% for M331. M372 was detected at 27.2%. At the c-terminus, residues M488, M489, and M492 were found in the same peptide sequence with an overall oxidation of 67.2%. The last methionine (M497) was not detected as oxidized.

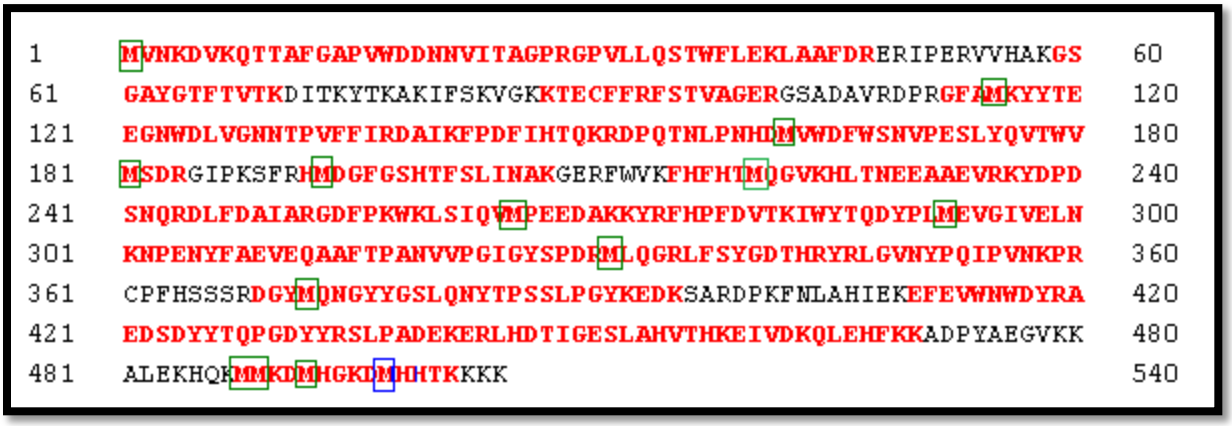

Figure 4.9. Msr oxidized with hydrogen peroxide which yields a 74.4% sequence coverage (red) with 13 methionines oxidized (green) and one methionine unoxidized (blue).

Mutant *msr* (*msr*) in PBS was detected with 59.7% sequence coverage, with 9 out of the 14 methionine found (Figure 4.10). M115 was detected with 35.8% oxidation. M193 had approximately 48% oxidation. M220 was found with 61.2% oxidation. M265 was partially digested into three peptides with the following oxidation with increasing missed cleavages:

16.0%, 41.2%, and 10.1%. M331 is detected at 26.4% oxidation. All four residues (M488, M489, M492, and M497) as one peptide chain from the C-terminus were detected with an oxidation of 37.9%.

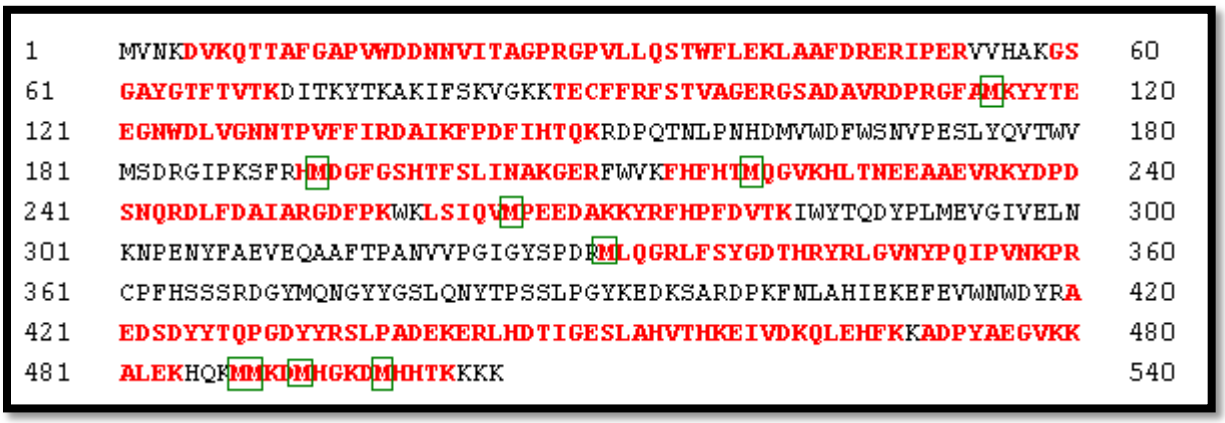

Figure 4.10. *msr* with PBS is detected with 59.7% sequence coverage (red) with all 9 methionine detected as oxidized (green).

Msr mutant oxidized with HOCl was detected to have sequence coverage of 39.5% with 10 of the 14 methionines detected (Figure 4.11). M1 was only detected in its unoxidized form. M115 was detected 96.0% oxidized. M193 was detected at 45.6% oxidation. M265 was partially digested into three peptides with oxidations of 17.5%, 36.1%, and 12.8%. M331 was found to have an oxidation of 51.8%. M372 was detected at 24.1% oxidation. Trypsin digestion did not completely cleave these four methionines (M488, M489, M492, and M497) but kept them as one peptide sequence where the total oxidation of 35.6%.

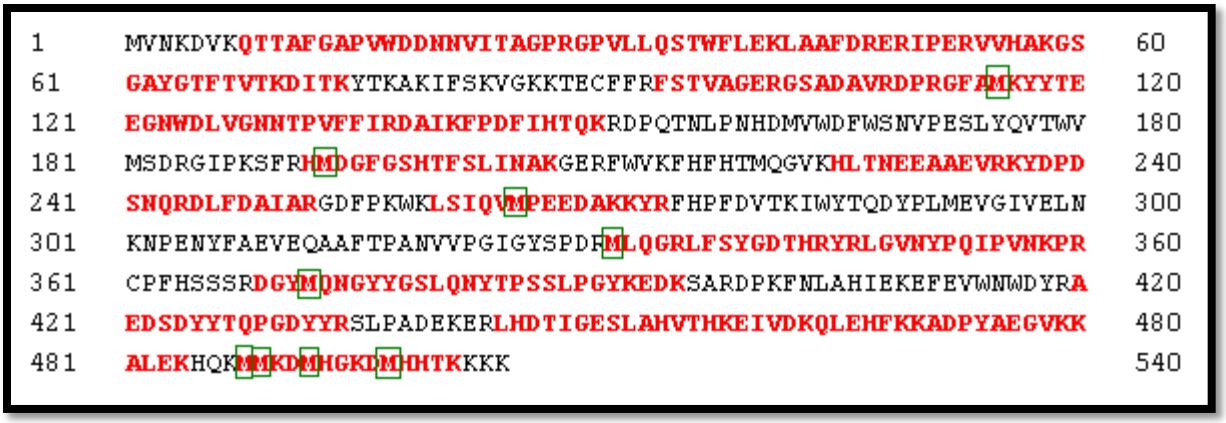

Figure 4.11. *msr* oxidized with HOCl yields a 39.5% sequence coverage (red) with all the methionines detected as oxidized (green).

As seen in Figure 4.12, the mutant msr was oxidized with hydrogen peroxide yielded 47.1% sequence coverage with 6 of the 14 methionines detected. There were no N-terminal residues observed. At M193 there were no oxidation detected. M265 was partially digested into two peptides with oxidation of 28.6% and 20.3%. M331was detected at 60.1% oxidation. The C-terminal residues (M488, M489, and M492) were detected to be fully oxidized.

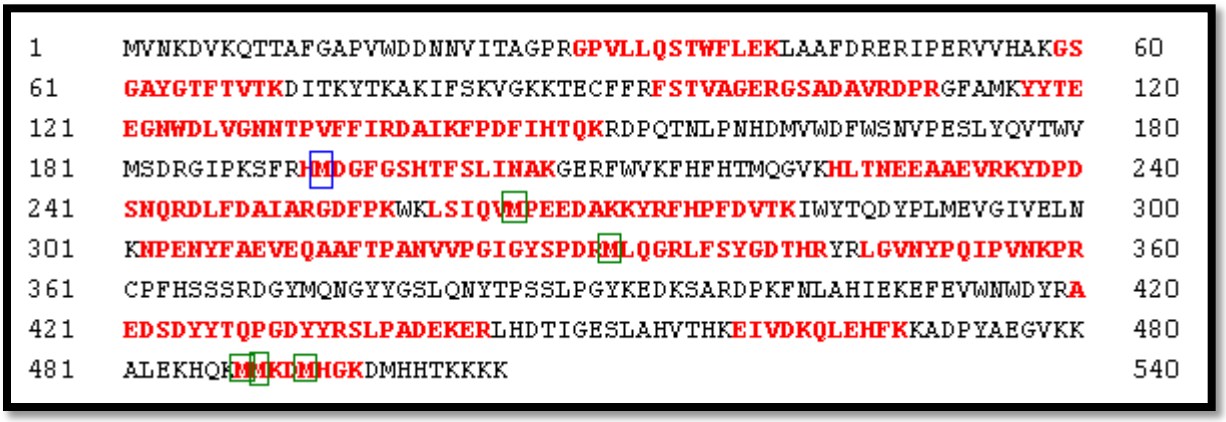

Figure 4.12. *msr* oxidized with hydrogen peroxide was detected with a sequence coverage of 47.1% (red) with five methionines oxidized (green) and one methionine at M192 unoxidized (blue).

Table 4.2. Oxidation levels of Wild Type strain (Msr) vs. mutant strains (*msr*) with various exposures to different oxidants

Met	**Sample**	**[oxidized]/ [total]**	**Standard Dev**		**Met**	**Sample**	**[oxidized] /[total]**	**Standard Dev**
265	*msr* H2O2	0.112	0.027		**331**	*msr* H2O2	0.761	0.043
	msr HOCl	0.105	0.016			*msr* HOCl	0.783	0.101
	msr PBS	0.051	0.010			*msr* PBS	0.408	0.135
	SS1 H2O2	0.128	0.009			*SS1* H2O2	0.282	0.056
	SS1 HOCl	0.208	0.013			*SS1* HOCl	0.364	0.045
115	*msr* H2O2	0.526	0.156		**1**	*msr* H2O2	0.157	0.063
	msr HOCl	0.629	0.030			*msr* HOCl	0.147	0.038
	msr PBS	0.248	0.004			*msr* PBS	ND	ND
	SS1 H2O2	0.055	0.014			*SS1* H2O2	ND	ND
	SS1 HOCl	0.241	0.034			*SS1* HOCl	0.205	0.057
372	*msr* H2O2	0.293	0.058		**497**	*msr* H2O2	ND	ND
	msr HOCl	0.203	0.045			*msr* HOCl	ND	ND
	msr PBS	0.261	0.069			*msr* PBS	0.762	0.006
	SS1 H2O2	0.331	0.122			*SS1* H2O2	ND	ND
	SS1 HOCl	0.280	0.084			*SS1* HOCl	0.559	0.047

Conclusions

As seen in Table 4.1., five methionines were able to provide some insight of Msr having the role of repairing damaged Met(O) to its native form. As seen in methionine residues M115 and M497, the amount of oxidation decreased when Msr was added to the oxidized catalase. This suggests that Msr does take the role of repairing the damaged methionine thus decreasing the overall level of oxidation. The results for the *in vitro* experiment were not concrete and many other changes were made for a more credible result. The major problem that arose from this experiment was the reproducibility of sequence coverage from the sample due to the inherent inconsistencies of packing individual nanofrit columns. This process was very time consuming and not very efficient for a high throughput analysis. Inconsistencies of packing were apparent from one column to another. The column packing often caused the appearance of poor peak shapes due to the interference from other peptides or chemical noise. Thus the quantitations of

fraction oxidized for each methionine residues were not consistent. As an example, a single experimental run would provide a percentage of sequence coverage with two thirds of the targeted methionine residues and data good enough for quantitation. On the other hand as the second experimental run was analyzed, a significant decrease in overall sequence coverage was observed. The targeted methionine residues were also reduced to less than a third of the methionine residues detected. Despite the inconsistencies and irreproducible data, data dependant acquisitions provided some quantitative data about oxidation and repair. This method provided enough data for extraction of precursor and product ions of specific m/z correlating to the peptide sequence containing the targeted methionine residues. These set of data has also provided an insight of where the unoxidized and oxidized peptides eluted and fragmented. To solve for the inconsistencies in sequence coverage and the identification of the oxidized methionines in this experiment, the future experiments will use a new column and source provided by Michrom Bioresources.

The second half of this chapter continues studying the effects of different catalase strain in an *in vivo* environment. Wild type strain (Msr) was compared to mutant strain (*msr*) for any detection of changes in levels of oxidation. Given that the nanofrit columns had poor reproducibility, a new column and source was installed onto the LTQ (Michrom Bioresources, Inc.). As seen in Table 4.2, the difference between the wild type strains (Msr) and the mutant strain (*msr*) agrees with our hypothesis that the oxidation increased because the mutant strain was more susceptible to treatments of oxidants. Similar trends were also exhibited in the catalase activity experiment involving the same samples (Figure 4.13). The catalase activity of the wild type strain exhibited higher levels of activity unlike the mutant strain. The difference between the two oxidants (HOCl and H_2O_2) can also be taken into account as HOCl causes more

damage thus losing more activity in the catalase strain. With the use of the Michrom column, time spent bomb loading nanofrit columns have been eliminated and results are more reproducible. However, there is still the issue of unaccounted peaks appearing in the RAW data files. The data from the *in vivo* was taken into account and a different method was produced and used in all further experiments. The different technique, pseudo-MRM, should increase the intensities of the unoxidized and oxidized peaks, thus providing an accurate peak area for a more precise calculation at each methionine residues.

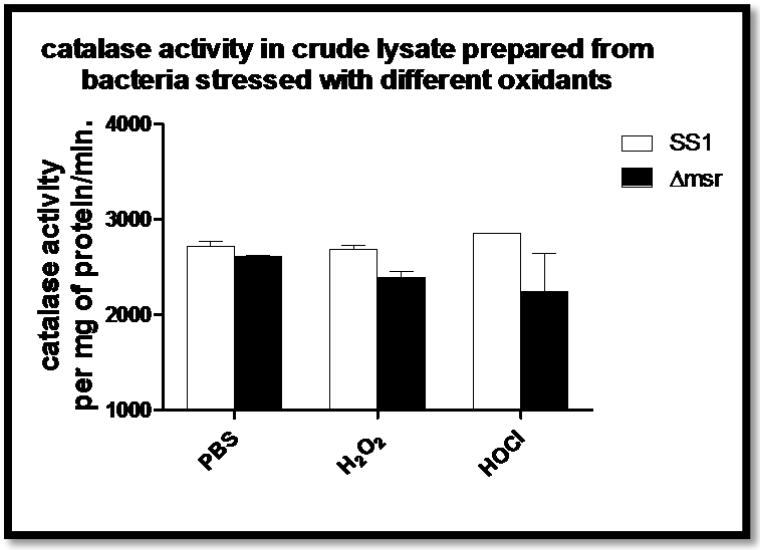

Figure 4.13. Catalase activity of wild type strain (white) and mutant strain (black) treated with H_2O_2 and HOCl. A decrease in catalase activity is illustrated in the mutant strain compared to the wild type strain.

CHAPTER 5

MS PSEUDO-MRM

Pseudo-MRM on LTQ

As reported in Chapter 4, data dependant acquisition was unable to produce reliable results especially in reproducibility of sequence coverage from one experimental run to another. A new source, ADVANCE™ CaptiveSpray™ (Michrom Bioresources), provided reproducible uninterrupted flow, an improvement in sensitivity, and allowed for higher flow rates. Another difference between the old setup versus the new Michrom setup was detected in the shape of the spray. The ADVANCE source focused the spray directly into the mass spectrometer source, unlike the previous setup where the spray was inconsistent and unfocused. The results of an unfocused spray lead to loss of sample as well as poor sensitivity. Coupled with the new source, the Magic C-18 column (Michrom Bioresources) replaced nanofrit columns. The new changes corrected some of the problems such as reproducibility within a triplicate run in addition with acquiring reliable sequence coverage. However, even with these new changes, there still exists one major issue. The fragment ions in the MS/MS spectra generates very low signal-to-noise ratio. A different method, pseudo-MRM, was developed to improve the signal-to-noise ratio for better quantitation of the unoxidized and oxidized m/z peaks.

Table 5.1. Precursor and product ion of catalase with trypsin digest

Met Residue	Precursor ion m/z unoxidized	Precursor ion m/z oxidized	Product ion m/z unoxidized	Product ion m/z oxidized
1	417.23	425.23	473.24	489.25
115	277.1	294.13	278.1	294.1
162	1337.14	1342.47	1149.12	1157.04
181	1137.14	1347.8	1149.12	1165.2
193	587.91	593.24	485.8	493.8
220	411.21	416.90	465.37	473.30
265	680.35	688.36	819.36	835.36
265	744.27	752.27	947.32	963.32
292	1156.1	1164.1	1341.7	1357.7
331	561.95	566.28	585.23	585.23
372	902.31	907.64	848.36	848.36
489	489.21	497.21	803.32	819.32
490	489.21	505.21	803.32	835.32
493	489.21	513.21	803.32	841.32
W17	1115.2	1123.2	1553.63	1569.64

Table 5.2. Precursor and product ion of catalase with Asp-N digest

Met Residue	Precursor ion m/z unox	Precursor ion m/z ox	Product ion m/z unox	Product ion m/z ox
W17	711.28	719.28	401.25	417.25
M331	722.09	730.09	664.59	672.59
M265	924.1	932.1	1473.78	1489.78
M115	982.4	990.4	925.55	933.55
M181	1095	1103	1439.58	1455.58
M489,490	787.45	792.78	749.42	754.75
M489, 490	787.45	798.11	749.42	760.08
M372	1416.8	1424.8	977.54	977.54
M292	1495	1500.33	1607.36	1615.36

The MS spectra from the data dependant acquisition methods were used to determine the precursor and product ions of specific m/z which consisted of targeted methionine residues for both the trypsin digest (Table 5.1) and AspN digest (Table 5.2). The precursor ions from Table 5.1 were placed into an include list which can be found in the method setup of the LTQ XCalibur software. Without the include list, the ion trap will scan all ions for the precursor ions. The ions were isolated and fragmented for MS/MS analysis. The addition of an include list as part of the

method forces the LTQ to skip ions not on the include list in the scanning process and only isolate the ions that are present on the list. The ions were later fragmented and ejected into the detector. A separate method was created using the precursor ions from Table 5.2 for Asp-N digestion. By excluding all other peaks in the scan, the pseudo-MRM technique will not only increase reproducibility from multiple runs but also the intensities of each precursor peak. The raw files were then manually analyzed on the analytical software, XCalibur Qual Browser V1.4. The product ions from Tables 5.1 and 5.2 were inputted into the program to the respective precursor ions. The intensities of the precursor ion peak will increase by including the product ions in the analytical software. Figure 5.1 displays a couple of base peak chromatogram depicting the difference between data dependant acquisition and the pseudo-MRM technique. As seen in the Figure 5.1.A, the oxidized peak has a width of approximately three minutes due to the co-elution of peptides and contaminants of overlapping m/z. However, in Figure 5.1.B, the oxidized peak was decreased to half a minute. The signal-to-noise ratios have increased dramatically as the peak width becomes sharper and the background decreases. A wider peak width usually suggests other abundant peaks are the main reason for lower intensities seen in the data dependant acquisition. The fraction oxidized, Equation 4.1, were calculated for each precursor m/z containing the targeted methionine residue.

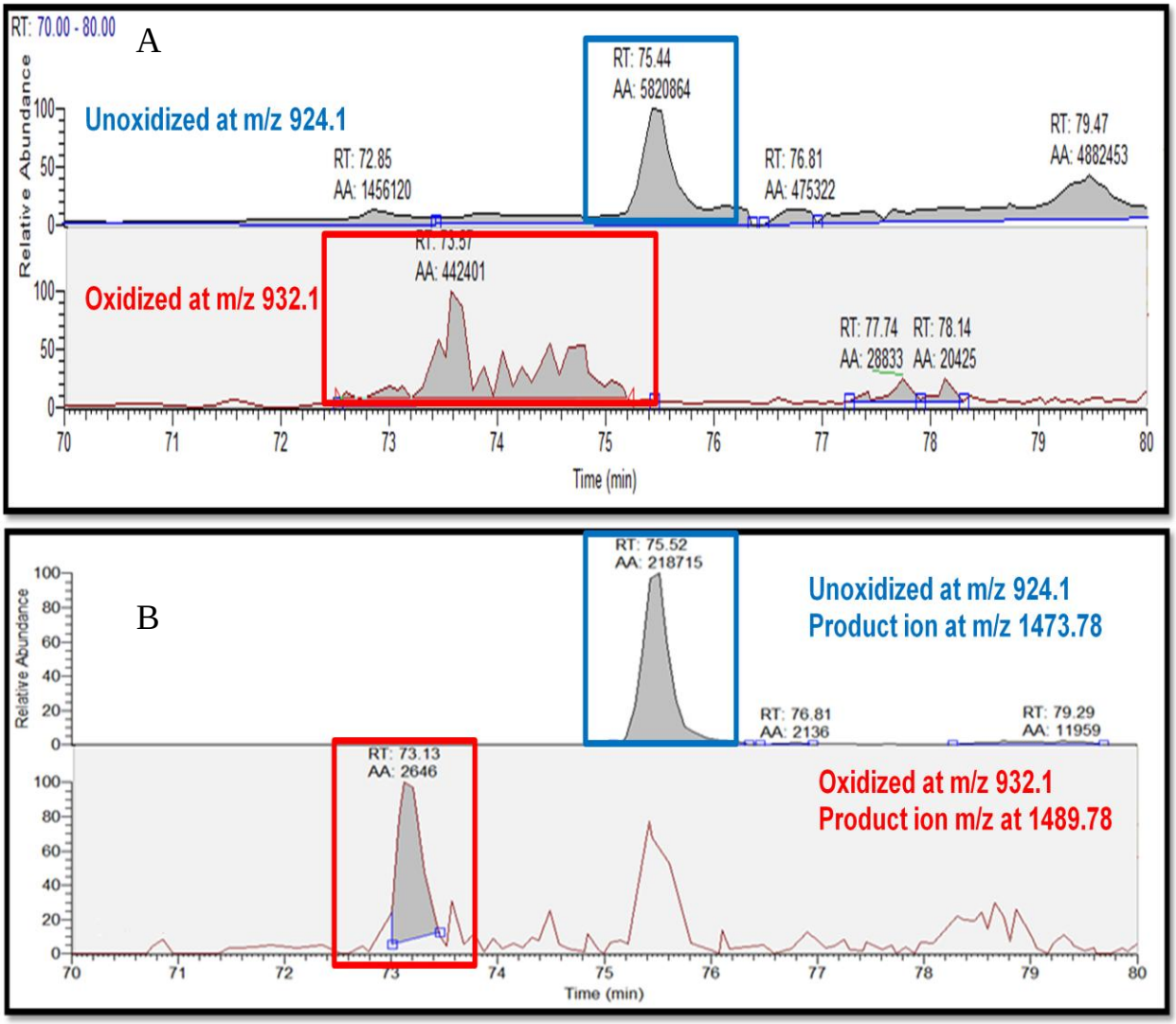

Figure 5.1. Catalase oxidized with Chloramine-T comparing base peak chromatogram in Data Dependant acquisition versus Pseudo-MRM analysis. A) Data dependant acquisition analysis at precursor ions of M265: unoxidized peak at m/z 924.1 and oxidized at m/z 932.1. B) Pseudo-MRM analysis of M265: unoxidized M265 with a precursor of m/z 924.1 with a product ion of m/z 1473.78 and oxidized M265 with a precursor of m/z 932.1 and a corresponding product ion of m/z 1489.78.

The protocols used in the pseudo-MRM experiment can be referred to Chapter 2: pseudo-MRM protocol. Briefly, the catalase samples were isolated, purified, and then treated with excess molar concentration of HOCl or ChT. It is then quenched with excess methionines. The samples were either digested with a sequence grade trypsin or with endoproteinase Asp-N. A different digestion protocol was introduced to catalase for identification of methionine residues

that were not detected with a trypsin digest. However, by cleaving the catalase at the N-terminal of aspartic acid with asp-N, this will allow identification of some of the methionine residues that couldn't be detected in the trypsin digest.

Results

The first experiment revisits the CD analysis of oxidized catalase with different molar excess of HOCl (Figure 3.2). These same samples were analyzed with the pseudo-MRM technique. Shown in Figure 5.2, trypsin digest of the four samples were analyzed: unoxidized catalase, 30x molar excess HOCl, 60x molar excess HOCl, and 100x molar excess HOCl. The oxidation signal was intense and produced good signals for the detected methionines. The fraction oxidized was calculated for each methionine residues at different molar excess of oxidants. Partial digestion could hinder the peptide sequence from being fully oxidized similar to its fully digested counterpart. The absence of 100x molar excess of HOCl from M220 could suggest that this methionine residue is still folded or not accessible to the oxidants as easily as the low dosage of oxidants.

The varying amounts of oxidized catalase were digested with the asp-N protocol and analyzed with the pseudo-MRM technique (Figure 5.3). Digestion with trypsin did not always include certain methionine residues such as M115 and M331. However, with the new asp-N digestion protocol, methionine residues such as M115 and M331 were detected. Other methionine residues such as M265, M292, and M372 were reproducible in both trypsin and asp-N digest.

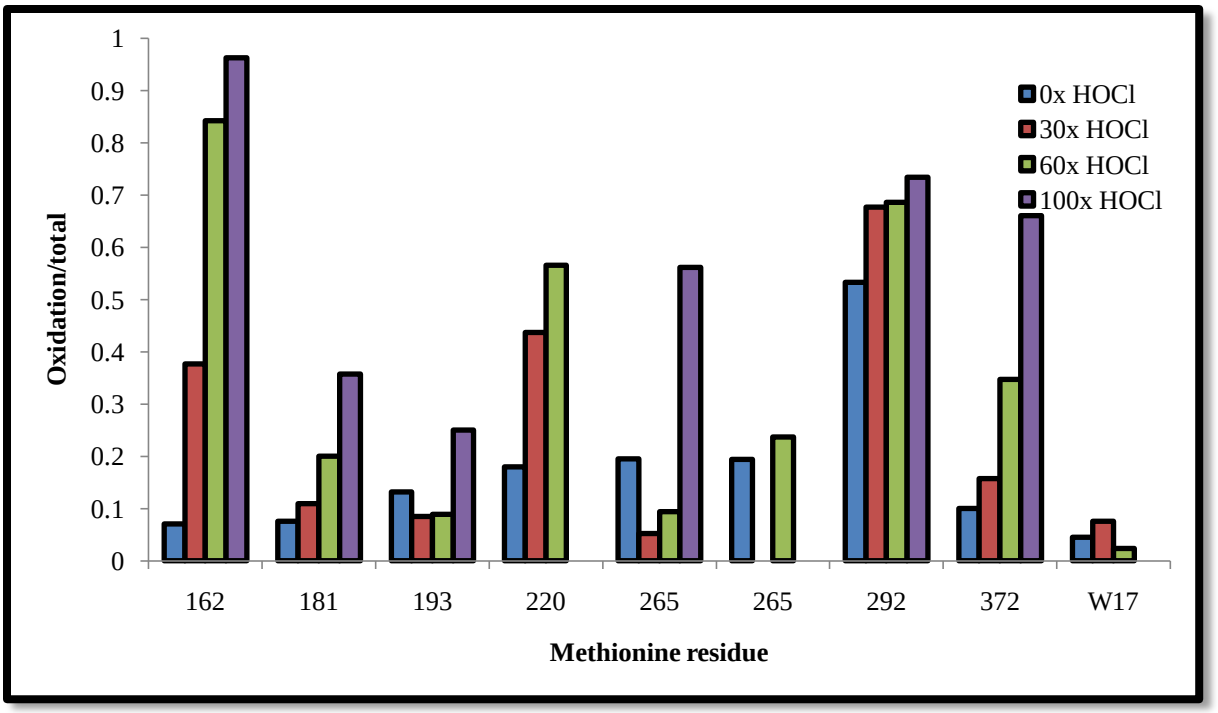

Figure 5.2. Fraction oxidized of specific methionine residues with increasing amounts of excess molar of HOCl [0x (blue), 30x (red), 60x (green), and 100x (purple)] with a trypsin digestion protocol. The analysis of a tryptophan residue was used as a standard peptide that should not be oxidized by HOCl.

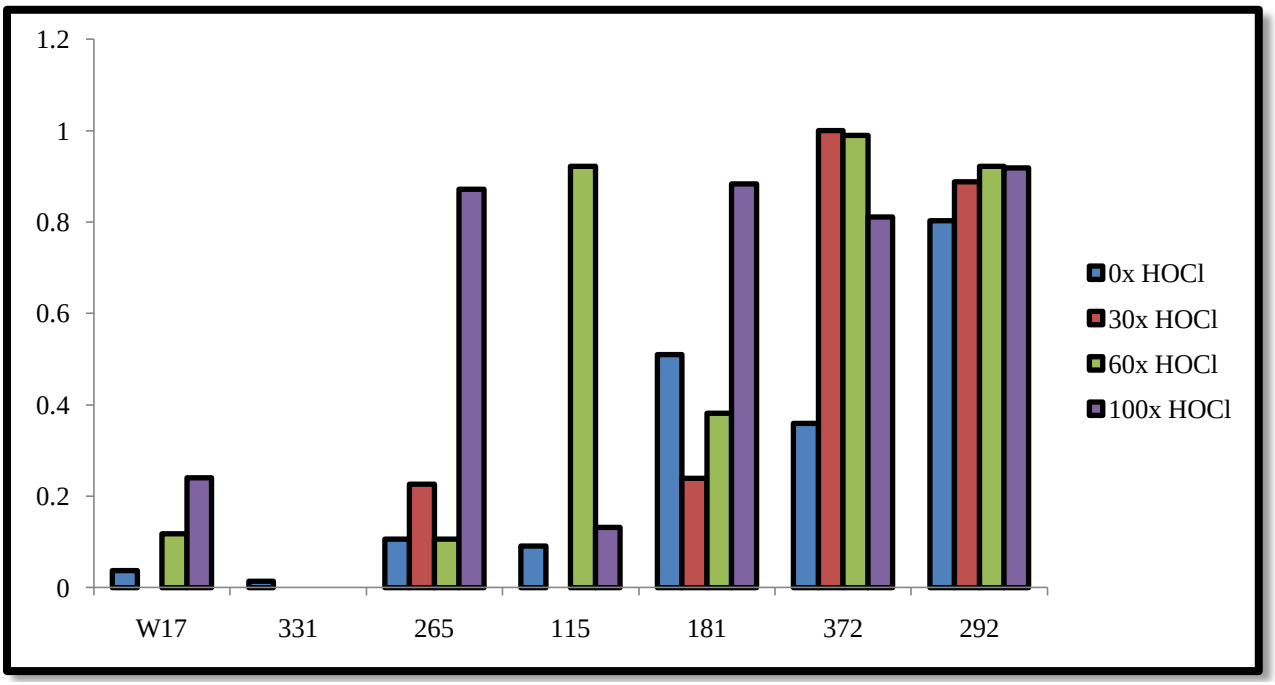

Figure 5.3. Single replicate of catalase treated with varying concentration of HOCl with AspN digest: 0x molar excess HOCl (blue), 30x molar excess HOCl (red), 60x molar excess HOCl (green), and 100x molar excess HOCl (purple)

Chloramine-T is another strong oxidant very similar to hypochlorous acid. The introduction of another oxidant was used to verify if any other oxidants will quantitatively produce similar results to HOCl-induced catalase. Single replicate of Chloramine-T (ChT) samples was collected using the pseudo-MRM method (Figure 5.4). The results were very similar to the HOCl catalase samples (Figure 5.2) with the same trend of increasing oxidants as well as an increased in the fraction oxidized of each methionine residues. Oxidation signals were also intense and produced good signals for the detected methionines. The response of chloramine-T was highly dose dependant with the exception of M193 which showed relatively little oxidation at all concentrations. The same was also seen in Figure 5.2 for M193 with presence of oxidation but not with any significant increase. Another digestion protocol was treated with asp-N and shown in Figure 5.5. The optimal amount of oxidation for further asp-N experiment seems to be 100x molar concentration. Similar to Figure 5.3 with the varying HOCl experiment digested with asp-N, this endoproteinase was able to detect methionine residues of M115 and M331 which were not detectable with trypsin digest. Methionine residues M181, M265, M372, and M292 were detected in both trypsin and asp-N digest suggesting these methionine residues are reproducible.

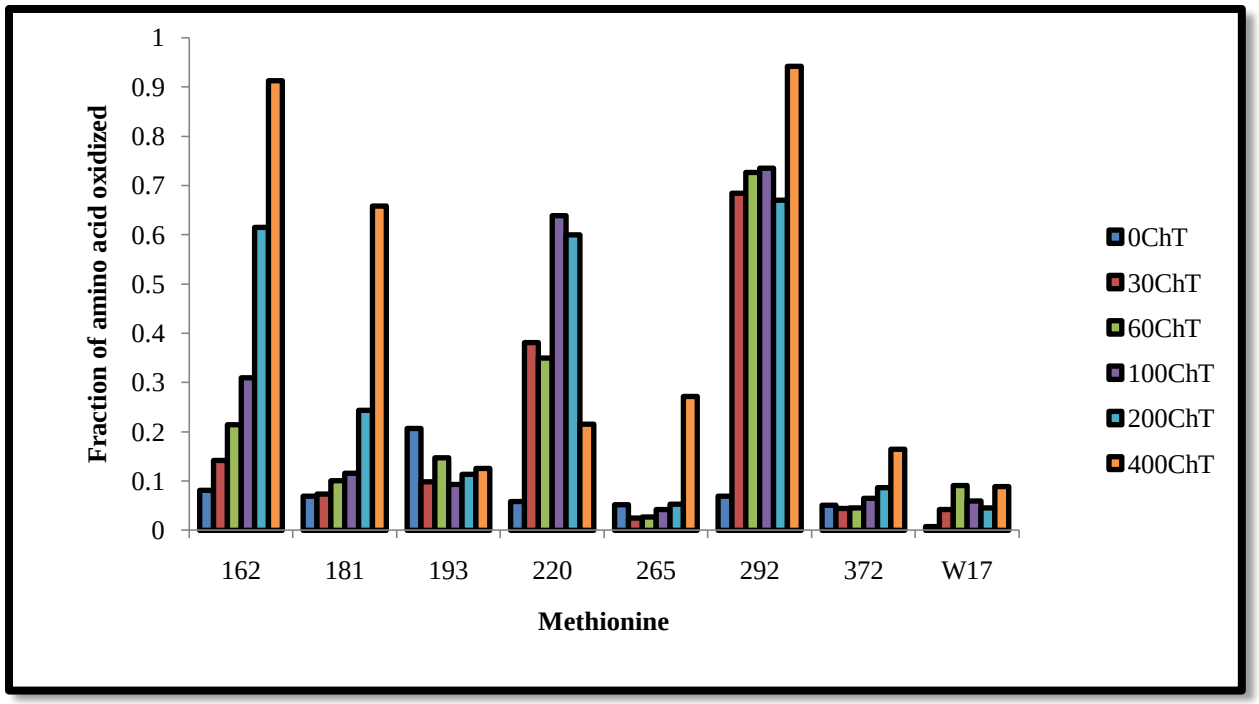

Figure 5.4. Single replicate of catalase sample treated with molar excess of Chloramine-T with trypsin digest: 0x (blue), 30x (red), 60x (green), 100x (purple), 200x (light blue), and 400x (orange).

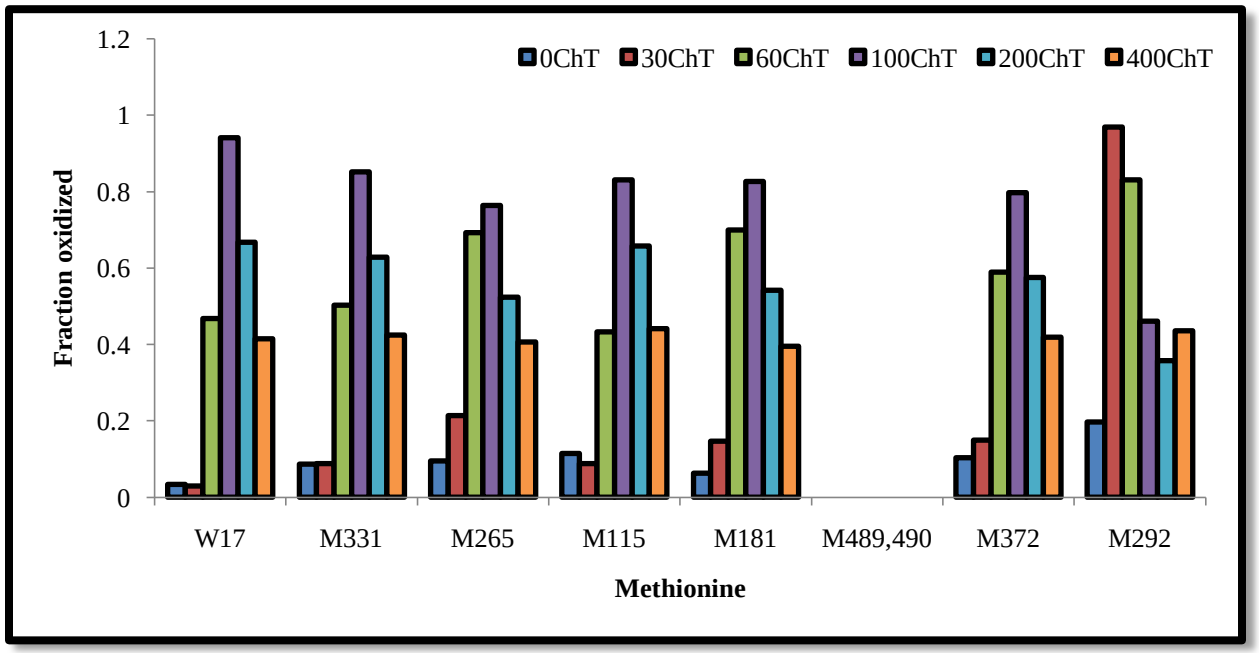

Figure 5.5. Single replicate of catalase treated with varying concentration of Chloramine-T: 0x (blue), 30x (red), 60x (green), 100x (purple), 200x (light blue), and 400x (orange) digested in AspN

The final set of experiments analyzed the treatment of Msr upon oxidized catalase for both trypsin (Figure 5.6) and asp-N digests (Figure 5.7). Figure 5.6 exhibited a similar trend in all methionine residues which included the unoxidized catalase having very low oxidation percentages. The oxidized catalase was then treated with Msr for any indication of a decrease or increase in oxidation. As expected, there were insignificant changes between the unoxidized catalase to the msr treatment to the unoxidized catalase. The catalase was then treated with either HOCl or ChT. The two different oxidants yielded a high percentage of oxidation for the oxidized catalase. Interestingly, once Msr was introduced to the two oxidized catalase, the percentage of oxidation for the two samples were reduced significantly. As previously mentioned, trypsin digest does not cover all the methionine residues. However, the addition of another digestion protocol with asp-N, detection of the missing methionine residues was analyzed (Figure 5.7). Similar trends explained with the trypsin digest can be found with the asp-N digest. Some of the methionine residues that were not detected in trypsin but in the asp-N digest includes M331, M115, M489, and M490. Also M181, M265, M292, and M373 were reproducible in both the trypsin digest as well as the asp-N digest.

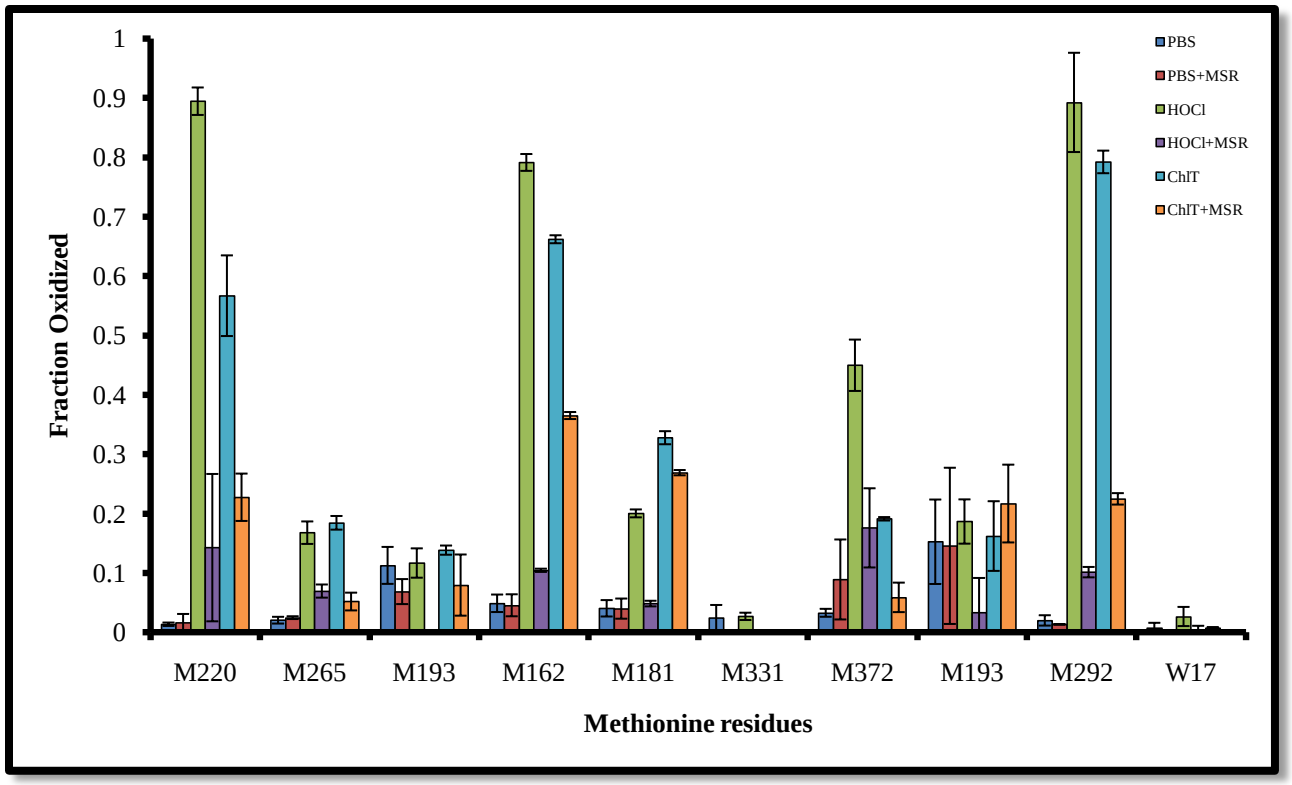

Figure 5.6. Catalase (dark blue) and oxidized catalase with HOCl (green) and ChT (light blue) treated with Msr: unoxidized catalase treated with Msr (maroon), HOCl induced catalase treated with Msr (purple), and ChT induced catalase treated with Msr (orange). All samples were digested with trypsin.

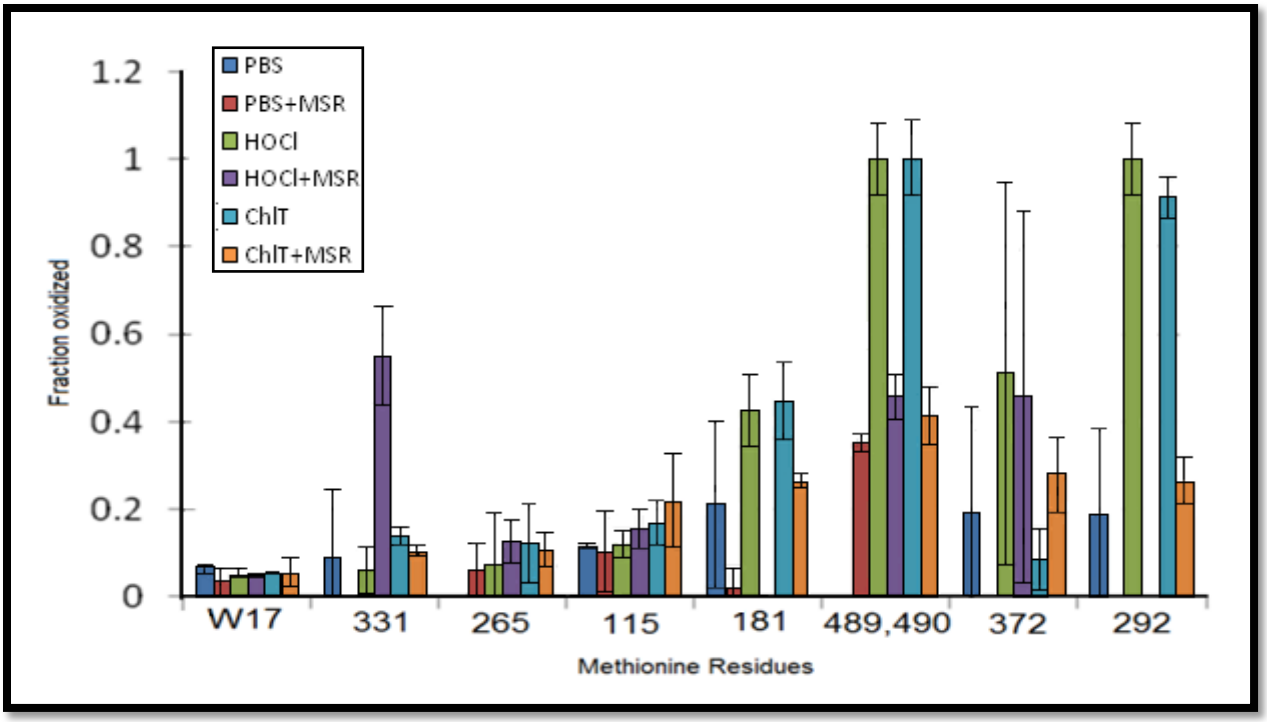

Figure 5.7. Catalase (dark blue) and oxidized catalase with HOCl (green) and ChT (light blue) treated with Msr: unoxidized catalase treated with Msr (maroon), HOCl induced catalase treated with Msr (purple), and ChT induced catalase treated with Msr (orange). All samples were digested with AspN.

Conclusion

By changing the mass spectrometer technique from a data dependant acquisition method to pseudo-MRM technique improved reproducibility within all samples. Table 5.1 and 5.2 were precursor and product ions extracted from the data dependant acquisition method and used as part of the pseudo-MRM technique. The pseudo-MRM technique decreased the abundant fragment ions that were suppressing the product ions signal-to-noise ratio needed to identify the correct methionine residues. Shown in Figures 5.2 to 5.5, the catalase was induced with increasing amounts of oxidants (HOCl and ChT) with different digests (trypsin and asp-N). The similarity between these four figures exhibited the reproducibility of reoccurring methionine residues. The same trend was repeated from one experiment to the other. Interestingly, the results from the catalase activity (Figure 3.4), CD (Figure 3.2), and LC-MS/MS (Figure 5.2) all

correlate perfectly together. As the catalase increase in oxidation, the catalase activity is decreased as well as the lost of structure was exhibited with a high percentage of oxidation calculated for each methionine containing peptide sequence.

The detection of 11 methionine residues of the 14 present in catalase amino acid sequence were analyzed with reproducible data seen in Figure 5.6. The trypsin digest was able to identify seven methionines successfully and was reproducible in a set of triplicate data. Asp-N digest was able to cover four additional methionine residues that were not detected in the trypsin digest (Figure 5.7). All methionines were oxidized except for the N- and C-terminal methionine residues (M1, M493, and M497). The remaining 11 methionines were targeted by oxidation and repaired by Msr as seen in both trypsin and asp-N digests. There was no evidence of selectivity towards certain methionines for repair. However, all methionine residues which were oxidized also became targets for repair. The surface of *H. pylori* catalase sequence was analyzed on a molecular graphing program, PyMol. Methionine residues 1, 220, 489, and 490 were all found located on the surface of the catalase sample. Except for M220, the other methionines were not detected as either oxidized or targeted for repair. The remaining 11 methionine residues were only detectable because trypsin and asp-N digest were successful.

CHAPTER 6

CONCLUSIONS

Helicobacter pylori is a bacterium found to cause stomach ulcers and chronic gastritis, which eventually leads to stomach cancer. However, under oxidative stress normally found in the body, this bacterium continues to survive and colonize. One way *Helicobacter pylori* protects itself from oxidative stress is by internally producing an enzyme called methionine sulfoxide reductase (Msr) which specifically targets and repairs oxidized methionine residues in a protein. Mass spectrometry was used as a different approach to analyze the role of Msr with Msr in *Helicobacter pylori* catalase.

In order to understand the role of Msr, the basics of qualitative and quantitative studies of an oxidized protein was performed. A biological assay (Figure 3.4) confirmed a significant decrease in catalase activity as the molar excess of HOCl increased. Circular dichroism confirmed the lost of catalase activity correlating with the loss of secondary structure (Figure 3.2). Mass spectrometry provided a quantitative way to calculate the percent of oxidation for each methionine containing peptide (Figure 5.2 – 5.3). The increase in fraction is associated to the loss of catalase activity as well as the loss of secondary structure.

The role of GroEL/ES in facilitating the refolding of protein while also restoring the activity was analyzed by both biological assay (Figure 3.5) and CD (Figure 3.3). The catalase activity of GroEL treatment increased significantly compared to the oxidized catalase, suggesting the possibility of protein refolding and restoration of protein activity. This was confirmed with CD scans exhibiting partial refolding of the oxidized catalase treated with GroEL.

Referring to Figure 3.5, the catalase activity was also analyzed for the interaction between catalase and Msr. Results from the catalase activity correlates with the pseudo-MRM results seen in Figure 5.6 and 5.7. The biological assay exhibited a significant decrease when the catalase was treated with excess HOCl. The catalase activity increased as Msr was treated to the oxidized catalase. The percent of oxidation exhibited similar trends for each methionine containing peptides when analyzing MS/MS data from pseudo-MRM technique. The treatment of excess Msr was introduced to the oxidized catalase and was analyzed to have a lower fraction oxidized at each specific methionine containing sequence.

The results from biological assays, CD, and MS/MS methods appear to be sufficiently reproducible in analyzing oxidized methionines along with identifying which residues were targeted by Msr. Eleven of the fourteen methionine residues were identified as targeted and repaired (Figure 6.1). The remaining three methionines were not detected due to its location at the C- and N-terminal of the protein. All experiments observed the role of Msr as a non-selective enzyme. This suggests that Msr will repair any oxidized methionine as long as the methionine containing peptide is solvent accessible. Sequence coverage as well as higher intensities in the chromatogram was also reproducible. Pseudo-MRM has opened the doors for future studies involving the identification of oxidized methionines for many other proteins.

Table 6.1 Methionine Residues Identified from Trypsin and AspN Digest

Met residue	Trypsin	AspN	Met residue	Trypsin	AspN
1			292	+	+
115		+	331		+
162	+		373	+	+
181	+	+	488		+
193	+		489		+
220	+		492		
265	+	+	497		

REFERENCES

1. Lin, M.T. and M.F. Beal, *Mitochondrial dysfunction and oxidative stress in neurodegenerative diseases.* Nature, 2006. **443**(7113): p. 787-795.

2. Brot, N. and H. Weissbach, *Peptide Methionine Sulfoxide Reductase: Biochemistry and Physiological Role.* Biopolymers (Peptide Science), 2000. **55**: p. 288-296.

3. Alamuri, P. and R.J. Maier, *Methionine sulphoxide reductase is an important antioxidant enzyme in the gastric pathogen Helicobacter pylori.* Molecular Microbiology, 2004. **53**(5): p. 1397-1406.

4. Dunn, B., H. Cohen, and M. Blaser, *Helicobacter pylori.* Clinical Microbiology Reviews, 1997. **10**(4): p. 720-741.

5. Correa, P., *Human gastric carcinogensis: a multistep and multifactorial process-first American Cancer Society Award lecture on cancer epidemiology and prevention.* Cancer Research, 1992. **52**: p. 6735-6740.

6. Akamatsu, T., et al., *Transmission of Helicobacter pylori infection via flexible fiberoptic endoscopy.* American Journal of Infection Control, 1996. **24**: p. 396-401.

7. Klein, P.D., et al., *Water source as risk factor for Helicobacter pylori infection in Peruvian childrean.* Lancet, 1991. **337**: p. 1503-1506.

8. Megraud, F., *Transmission of Helicobacter pylori: feacal-oral versus oral-oral route.* Alimentary Pharmacology & Therapeutics, 1995. **9**(2): p. 85-91.

9. Marshall, B.J. and J.R. Warren, *Unidentified curved bacilli in the stomach of patients with gastritis and peptic ulceration.* Lancet, 1984: p. 1311-5.

10. Mooney, C., et al., *Neutrophil activation by Helicobacter pylori.* Gut, 1991. **32**(8): p. 853-857.

11. Babior, B.M., *Oxygen-Dependent Microbial Killing by Phagocytes.* New England Journal of Medicine, 1978. **298**(12): p. 659-668.

12. Iyer, G., M. Islam, and J. Quastel, *Biochemical aspects of phagocytosis.* Nature, 1961. **192**: p. 535-541.

13. Hazell, S.L., A.G. Harris, and M.A. Trend, eds. *Evasion of the toxic effects of oxygen*. Helicobacter pylori: physiology and genetics, ed. H.L.T. Mobley, G.L. Mendz, and S.L. Hazell. 2001, ASM Press: Washington, D.C. 167-175.

14. Bagchi, D., G. Bhattachatya, and S.J. Stohs, *Production of reactive oxygen species by gastric cells in association with Helicobacter pylori.* Free Radical Research, 1996. **24**: p. 439-450.

15. Ramarao, N., S.D. Gray-Owen, and T.F. Meyer, *Helicobacter pylori induces but survives the extracellular release of oxygen radicals from professional phaocytes using its catalase activity.* Molecular Microbiology, 2000. **38**: p. 103-113.

16. R. W. Seyler, J., J.W. Olson, and R.J. Maier, *Superoxide dismutase-deficient mutants of Helicobacter pylori are hypersensitive to oxidative stress and defective in hose colonization.* Infection and Immunity, 2001. **69**: p. 4034-4040.

17. Wang, G., et al., *Role of a Bacterial Organic Hydroperoxide Detoxification System in Preventing Catalase Inactivation.* Journal of Biological Chemistry, 2004. **279**(50): p. 51908-51914.

18. Hazell, S.L., D.J. Evans, Jr, and D.Y. Graham, *Helicobacter pylori catalase.* J Gen Microbiol, 1991. **137**(1): p. 57-61.

19. Pattison, D.I. and M.J. Davies, *Absolute Rate Constants for the Reaction of Hypochlorous Acid with Protein Side Chains and Peptide Bonds.* Chemical Research in Toxicology, 2001. **14**(10): p. 1453-1464.

20. Weissbach, H., et al., *Peptide Methionine Sulfoxide Reductase: Structure, Mechanism of Action, and Biological Function.* Biochemistry and Biophysics, 2002. **397**(2): p. 172-178.

21. Hawkins, C.L., D.I. Pattison, and M.J. Davies, *Hypochlorite-induced oxidation of amino acids, peptides and proteins.* Amino Acids, 2003. **25**(3): p. 259-274.

22. Kim, Y.H., et al., *Comparing the effect on protein stability of methionine oxidation versus mutagenesis: steps toward engineering oxidative resistance in proteins.* Protein Engineering, 2001. **14**(5): p. 343-347.

23. Alamuri, P. and R.J. Maier, *Methionine Sulfoxide Reductase in Helicobacter pylori: Interaction with Methionine-Rich Proteins and Stress-Induced Expression.* Journal of Bacteriology, 2006. **188**(16): p. 5839-5850.

24. Ezraty, B., L. Aussel, and F. Barras, *Methionine sulfoxide reductases in prokaryotes.* Biochemica et Biophysica Acta, 2004. **1703**: p. 221-229.

25. Sharov, V.S., et al., *Diastereoselevtive reduction of protein-bound methionine sulfoxide by methionine sulfoxide reductase.* FEBS Letters, 2001. **455**: p. 247-250.

26. Grimaud, R., et al., *Repair of oxidized proteins: Identification of a new methionine sulfoxide reductase.* Journal of Biological Chemistry, 2001. **276**(52): p. 48915-48920.

27. Moskovitz, J., et al., *Chromosomal localization of the mammalian peptide-methionine sulfoxide reductase gene and its differential expression in various tissues.* Proceedings of

the National Academy of Sciences of the United States of America, 1996. **93**(8): p. 3205-3208.

28. Brot, N., et al., *Enzymatic reduction of protein-bound methionine sulfoxide.* Proceedings of the National Academy of Sciences of the United States of America, 1981. **78**(4): p. 2155-2158.

29. Caldwell, P., et al., *Oxidation of the methionine residues of Escherichia coli ribosomal protein L12 decreases the protein's biological activity.* Proceedings of the National Academy of Sciences of the United States of America, 1978. **75**(11): p. 5349-5352.

30. Fakunding, J.L., R.R. Traut, and J.W.B. Hershey, *Dependence of Initiation Factor IF-2 Activity on Proteins L7 and L12 from Escherichia coli 50 S Ribosomes.* Journal of Biological Chemistry, 1973. **248**(24): p. 8555-8559.

31. Kay, A., G. Sander, and M. Grunberg-Manago, *Effect of ribosomal protein L12 upon initiation factor IF-2 activities.* Biochemical and Biophysical Research Communications, 1973. **51**(4): p. 979-986.

32. Lockwood, A.H., et al., *The Role of Ribosomal Proteins L7 and L12 in Polypeptide Chain Initiation in Escherichia coli.* Journal of Biological Chemistry, 1974. **249**(4): p. 1213-1218.

33. Mazumder, R., *Effect of Thiostrepton on Recycling of Escherichia coli Initiation Factor 2.* Proceedings of the National Academy of Sciences of the United States of America, 1973. **70**(7): p. 1939-1942.

34. Hamel, E., M. Koka, and T. Nakamoto, *Requirement of an Escherichia coli 50 S Ribosomal Protein Component for Effective Interaction of the Ribosome with T and G Factors and with Guanosine Triphosphate.* Journal of Biological Chemistry, 1972. **247**(3): p. 805-814.

35. Sander, G., R.C. Marsh, and A. Parmeggiani, *Isolation and characterization of two acidic proteins from the 50S subunit required for GTPase activities of both EF G and EF T.* Biochemical and Biophysical Research Communications, 1972. **47**(4): p. 866-873.

36. Brot, N., et al., *The Requirement for Ribosomal Proteins L7 and L12 in Peptide-Chain Termination.* Proceedings of the National Academy of Sciences of the United States of America, 1974. **71**(1): p. 89-92.

37. Dzionara, M., *Ribosomal proteins. Secondary structure of individual ribosomal proteins of E. coli studied by circular dichroism.* FEBS Letters, 1970. **8**(4): p. 197-200.

38. Möller, W., H. Castleman, and C.P. Terhorst, *Characterization of an acidic protein in 50 s ribosomes of E. coli.* FEBS Letters, 1970. **8**(4): p. 192-196.

39. Ejiri, S.-i., H. Weissbach, and N. Brot, *The purification of methionine sulfoxide reductase from Escherichia coli.* Analytical Biochemistry, 1980. **102**(2): p. 393-398.

40. Lowther, W.T., et al., *Thiol–disulfide exchange is involved in the catalytic mechanism of peptide methionine sulfoxide reductase.* Proceedings of the National Academy of Sciences of the United States of America, 2000. **97**(12): p. 6463-6468.

41. Kuschel, L., et al., *Molecular cloning and functional expression of a human peptide methionine sulfoxide reductase (hMsrA).* FEBS Letters, 1999. **456**(1): p. 17-21.

42. Moskovitz, J., et al., *Escherichia coli peptide methionine sulfoxide reductase gene: regulation of expression and role in protecting against oxidative damage.* J. Bacteriol., 1995. **177**(3): p. 502-507.

43. Levine, R.L., et al., *Methionine residues may protect proteins from critical oxidative damage.* Mechanisms of Ageing and Development, 1999. **107**(3): p. 323-332.

44. Stadtman, E.R., et al., *Cyclic oxidation and reduction of protein methionine residues is an important antioxidant mechanism.* Molecular and Cellular Biochemistry, 2002. **234**(1): p. 3-9.

45. Vogt, W., *Oxidation of methionyl residues in proteins: tools, targets, and reversal.* Free Radical Biology & Medicine, 1995. **18**: p. 93-105.

46. Ciorba, M.A., et al., *Modulation of potassium channel function by methionine oxidation and reduction.* Proceedings of the National Academy of Sciences of the United States of America, 1997. **94**(18): p. 9932-9937.

47. Hassouni, M.E., et al., *The minimal gene set member msrA, encoding peptide methionine sulfoxide reductase, is a virulence determinant of the plant pathogen Erwinia chrysanthemi.* Proceedings of the National Academy of Sciences of the United States of America, 1999. **96**(3): p. 887-892.

48. Moskovitz, J. and B.S. Berlett, *The yeast peptide - methionine sulfoxide reductase functions as an antioxidant in vivo.* Proceedings of the National Academy of Sciences of the United States of America, 1997. **94**: p. 9585-9589.

49. John, G.S., et al., *Peptide methionine sulfoxide reductase from Escherichia coli and Mycobacterium tuberculosis protects bacteria against oxidative damage from reactive nitrogen intermediates.* Proceedings of the National Academy of Sciences of the United States of America, 2001. **98**(17): p. 9901-9906.

50. Tomb, J.F., et al., *The complete genome sequence of the gastric pathogen Helicobacter pylori.* . Nature, 1997. **388**: p. 539-547.

51. Austin, J.W., et al., *Structural comparison of Urease and a GroEL analog from Helicobacter pylori.* Journal of Bacteriology, 1992(22): p. 7470-7473.

52. Dunn, A., M. Melville, and J. Frydman, *Review: cellular substrates of the eukaryotic chaperonin TRiC/CCT.* Journal of Structural Biology, 2001. **135**: p. 176-184.

53. Fenton, W.A. and A.L. Horwich, *Chaperonin-mediated protein folding: fate of substrate polypeptide.* Quarterly Reviews of Biophysics, 2003. **36**(02): p. 229-256.

54. Hartl, F.U., *Molecular chaperones in cellular protein folding.* Nature, 1996. **381**(6583): p. 571-580.

55. Hartl, F.U. and M. Hayer-Hartl, *Molecular Chaperones in the Cytosol: from Nascent Chain to Folded Protein.* Science, 2002. **295**(5561): p. 1852-1858.

56. Horwich, A.L., G.W. Farr, and W.A. Fenton, *GroEL−GroES-Mediated Protein Folding.* Chemical Reviews, 2006. **106**(5): p. 1917-1930.

57. Spiess, C., et al., *Mechanism of the eukaryotic chaperonin: protein folding in the chamber of secrets.* Trends in cell biology, 2004. **14**(11): p. 598-604.

58. Lin, Z. and H.S. Rye, *GroEL-Mediated Protein Folding: Making the Impossible, Possible*. Critical Reviews in Biochemistry and Molecular Biology, 2006. **41**(4): p. 211-239.

59. Braig, K., et al., *The crystal structure of the bacterial chaperonin GroEL at 2.8A.* Nature, 1994. **371**: p. 578-586.

60. Khor, H.K., M.T. Fisher, and C. Schoneich, *Potential Role of methionine Sulfoxide in the Inactivation of the Chaperone GroEL by Hypochlorous Acid (HOCl) and Peroxynitrite (ONOO-).* The Journal of Biological Chemistry, 2004. **279**(19): p. 19486-19493.

61. Netzer, W.J. and F. Ulrich Hartl, *Protein folding in the cytosol: chaperonin-dependent and -independent mechanisms.* Trends in biochemical sciences, 1998. **23**(2): p. 68-73.

62. Taylor, D.E., et al., *Genetic characterization of kanamycin resistance in Campylobacter coli.* Annales de l'Institut Pasteur / Microbiologie. **139**(6): p. 665-676.